A Supramolecular System for Quantifying Aromatic Stacking Interactions

Harry Adams,[a] Christopher A. Hunter,*[a] Kevin R. Lawson,[b] Julie Perkins,[a] Sharon E. Spey,[a] Christopher J. Urch,[b] and John M. Sanderson[a]

Abstract: A supramolecular complex for investigating the thermodynamic properties of intermolecular aromatic stacking interactions has been developed. The conformation of the complex is locked in a single well-defined conformation by an array of H-bonding interactions that force two aromatic rings on one end of the complex into a stacked geometry. Chemical double-mutant cycles have been used to measure an anthracene–aniline interaction ($+0.6 \pm 0.8$ kJ mol^{-1}) and a pentafluorophenyl–aniline interaction (-0.4 ± 0.9 kJ mol^{-1}) in this system. Although the interactions are very weak, the pentafluorophenyl interaction is attractive, whereas the anthracene interaction is repulsive; this is consistent with the dominance of π-electron electrostatic interactions. The nitropyrrole subunits used to control the conformation of these complexes lead to problems of aggregation and multiple conformational equilibria. The implications for the thermodynamic analysis are examined in detail, and the double-mutant-cycle approach is found to be remarkably robust with respect to such effects, since systematic errors in individual experiments are removed in a pair-wise fashion when the cycle is constructed.

Keywords: aromatic stacking · double-mutant cycle · hydrogen bonds · molecular recognition · pi interactions

Introduction

The process of molecular recognition is governed by noncovalent interactions, and the development of simple model systems to investigate the properties of these interactions has been a major thrust of research in supramolecular chemistry. One important class of intermolecular interactions is aromatic stacking.[1] The classic example is base stacking in DNA,[2–4] but stacking interactions between aromatic side chains are also found in proteins and play an important role in determining the fold of a protein and the substrate recognition properties.[5–7] Supramolecular chemists have exploited aromatic stacking interactions for substrate recognition by synthetic receptors and in template-directed synthesis of complex molecules.[9–20] The packing of aromatic molecules in the solid state, and hence the physical properties of these materials, is to some extent determined by stacking interactions.[21–24] Theoretical calculations have yielded some insight into the nature of aromatic interactions,[25–32] and there have been various attempts to quantify the interactions by using synthetic supramolecular systems.[33–38] Experimental data on the thermodynamics of noncovalent interactions are essential if we are to develop reliable computational methods for predicting the behaviour of complex molecular systems.[39–41] We have developed an experimental method for measuring intermolecular interactions using chemical double-mutant cycles, and this has been successfully applied to edge-to-face aromatic interactions.[42, 43] We present here the design and realisation of a supramolecular system for measuring aromatic stacking interactions.

[a] Prof. C. A. Hunter, H. Adams, J. Perkins, S. E. Spey, Dr. J. M. Sanderson
Centre for Chemical Biology
Krebs Institute for Biomolecular Science
Department of Chemistry, University of Sheffield
Sheffield S3 7HF (UK)
Fax: (+44) 114-273-8673
E-mail: c.hunter@sheffield.ac.uk

[b] Dr. K. R. Lawson, Dr. C. J. Urch
Zeneca Agrochemicals, Jealott's Hill Research Station
Bracknell, Berkshire, RG42 6ET (UK)

Results and Discussion

Design and Synthesis: The starting point for the development of a system to measure stacking interactions was the **1**·**2** complex previously used to measure edge-to-face interactions (Scheme 1).[43–46] To introduce stacking interactions into this system, the benzoyl rings must be rotated through 90°, so that they lie parallel to the aniline ring as shown in Scheme 2. Substituents *ortho* to the carbonyl group force such a conformation, so anthracene was chosen as it has such a large aromatic surface that the aniline ring will be forced to sit over it, even if the stacking interaction is repulsive.

We have previously used X-ray crystal structures of simple model compounds to probe the geometry of the terminal aromatic interaction in edge-to-face zipper complexes. For

  0947-6539/01/0722-4863 $ 17.50+.50/0

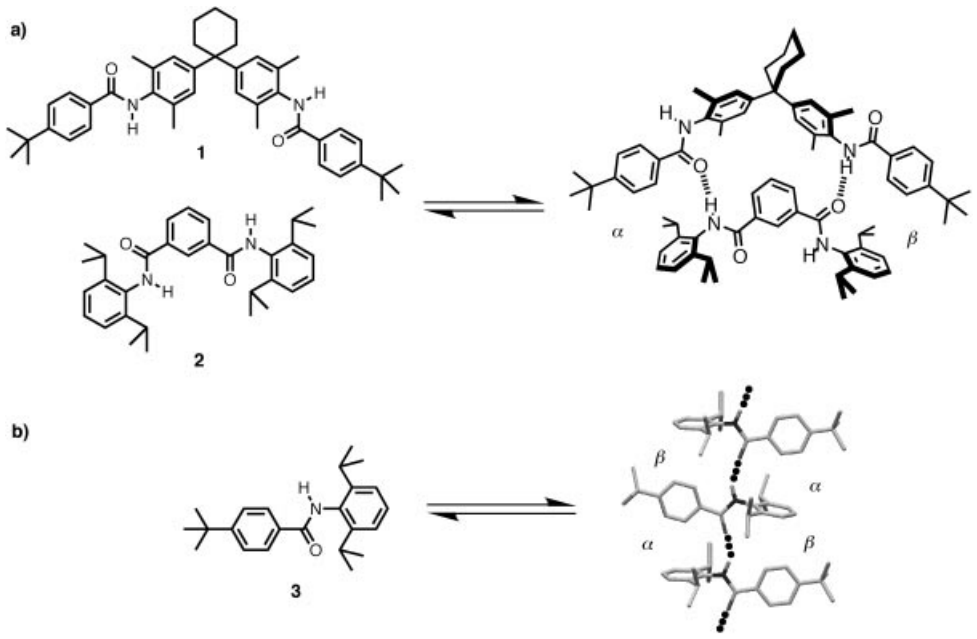

Scheme 1. a) Zipper complex **1·2** used to measure the terminal edge-to-face aromatic interaction in solution. b) Model compound **3** used to probe the geometry of this interaction in the solid state. Three molecules from the X-ray crystal structure of **3** are shown. The α and β interaction geometries are labelled.

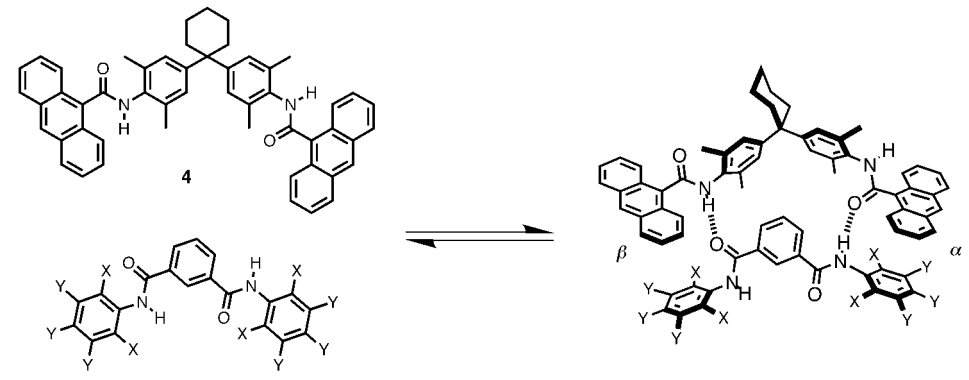

Scheme 2. Candidate complexes for measuring an aromatic stacking interaction.

example, **3** forms a H-bonded polymer with head-to-tail packing; this gives edge-to-face aromatic interactions throughout the structure (Scheme 1b). Closer examination of this structure reveals that there are actually two different aromatic interactions present: one in which the benzoyl carbonyl oxygen is a H-bond acceptor (α) and one in which the benzoyl amide is a H-bond donor (β). This difference is also manifest in different interactions on the two ends of the zipper complex in Scheme 1a.[43] Although the difference in the geometry of the edge-to-face interactions is very subtle, it becomes much more significant for stacking interactions. X-ray crystal structures of model compounds were used to probe the feasibility of the proposed aromatic stacking interactions in the complexes in Scheme 2. The coupling product **8** of 9-anthranoyl chloride and 2,6-diisopropylaniline was synthesised (Scheme 3) and crystallised. In the X-ray crystal structure, the molecules are arranged in H-bonded chains as expected, but there is a mixture of head-to-tail and head-to-head orientations (Scheme 4a). The aromatic rings are all approximately parallel, but the only true stacking interaction is an anthracene–anthracene interaction in the head-to-head pairs. The steric bulk of the isopropyl substituents prevents close parallel stacking of the anthracene with the aniline rings. Replacement of the isopropyl substituents with methyl groups (**9**, Scheme 3) removes the steric bulk, but in the crystal structure of this compound, the molecules all sit in a head-to-head arrangement with only anthracene–anthracene and aniline–aniline stacking interactions (Scheme 4b).

In an attempt to favour a head-to-tail arrangement, compound **10** was synthesised (Scheme 3), because the literature suggests that perfluorinated rings stack exceptionally well with hydrocarbon rings.[23, 24, 47, 48] A head-to-tail arrangement was indeed obtained, but the crystal structure showed three different aromatic interactions (Scheme 4c). By analogy with the structure of **3** in Scheme 1b, these interactions are labelled α, β1 and β2. The α interaction is the desired pentafluorophenyl–anthracene stacking interaction and involves a H-bond between the aniline amide NH and the anthracene carbonyl oxygen. In the two β interactions, the anthracene amide NH is the H-bond donor, and the aromatic rings are arranged in an edge-to-face geometry. In the head-to-tail packing arrangement, the β H-bond geometry does not allow aromatic stacking to take place: the aromatic rings must either be parallel and separated by about 5 Å, or they can be in close contact but not parallel. In contrast, the α H-bond geometry is perfectly adapted for aromatic stacking. This has important implications for the way in which these interactions are translated into the complexes in Scheme 2. Only the α H-bond geometry will result in a stacking interaction, and therefore we require unsymmetrical complexes, in which it is possible to control and distinguish the interactions on the α and β ends of the complex.

We have previously found that replacing the benzoyl group in the **1·2** complex with pyrrole gives rise to two bifurcated

  0947-6539/01/0722-4864 $ 17.50+.50/0

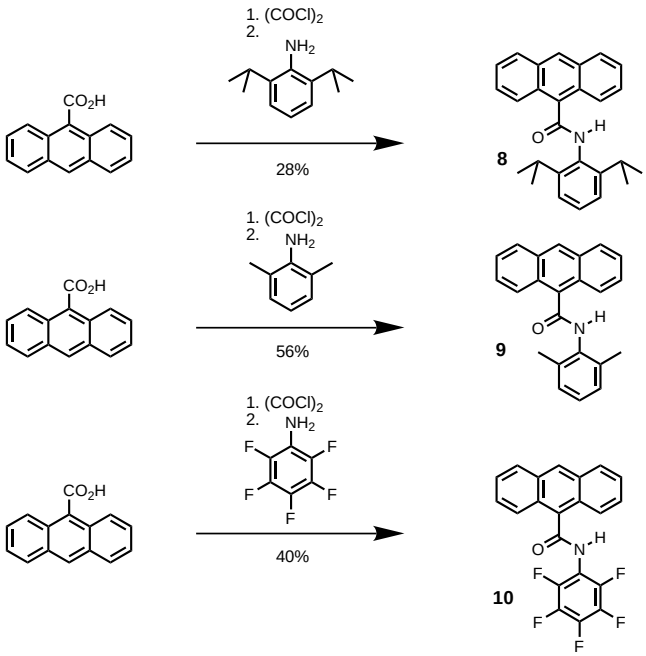

Scheme 3. Synthesis of the variously substituted compounds **8**, **9** and **10** in an attempt to regulate stacking in H-bonded chains.

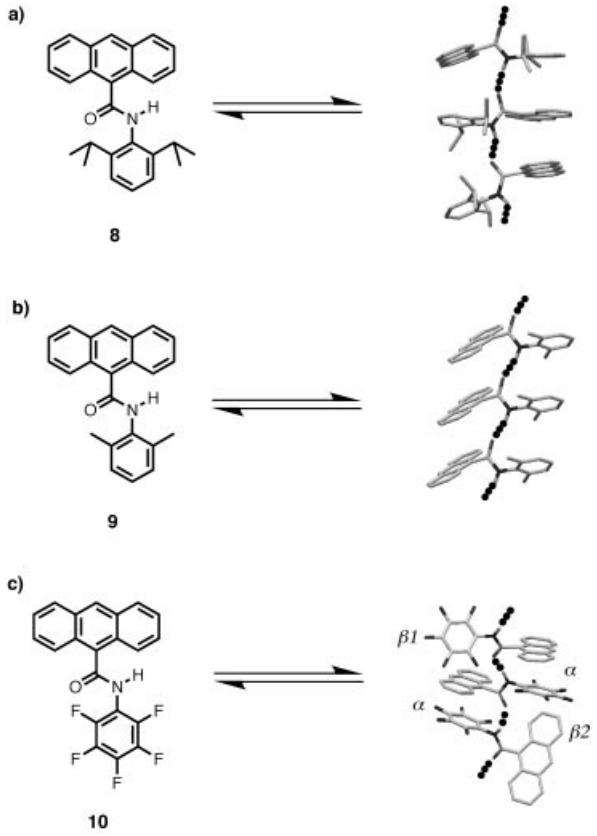

Scheme 4. a) Model compound **8** and the arrangement of three molecules in the X-ray crystal structure. Both head-to-tail and head-to-head arrangements of the aromatic substituents are observed. b) Model compound **9** and the arrangement of three molecules in the X-ray crystal structure. Only head-to-head interactions are found for the aromatic substituents. c) Model compound **10** with the arrangement of three molecules in the X-ray crystal structure. The molecules pack in a head-to-tail arrangement, giving the desired anthracene–aniline stacking interaction in the α geometry and edge-to-face interactions in the two β geometries.

H-bonds to the adjacent carbonyl oxygen, and this approach appears ideal for locking the conformation of the complex at the β end.[49] The principle is illustrated for the **11**·**7** complex in Scheme 5. When the anthracene–aniline interaction of interest is in the α geometry, there are two bifurcated H-bonds between the pyrrole and amide NH groups and the adjacent carbonyl oxygen; when the anthracene–aniline interaction is in the β geometry, there is only one H-bond between the aniline amide NH and the pyrrole carbonyl oxygen. This should significantly favour the conformation with the α stacking interaction over the β geometry in which the relevant aromatic rings are remote. We decided to bias the system further by incorporating a nitro group in the 4-position of the pyrrole to increase the H-bond donor strength of the pyrrole and amide NHs and stabilise the α conformation. Compounds **11** and **7** were synthesised according to Schemes 6 and 7, below. 4-Nitropyrrole-2-carbonyl chloride **15** was prepared according to a procedure described by Morgan and Morrey.[50] Mucobromic acid **12** was treated with sodium nitrite to form sodium malondialdehyde **13**[51] (Scheme 6). Condensation of **13** with glycine ethyl ester resulted in ethyl 4-nitropyrrole-2-carboxylate (**14**) which was subsequently hydrolysed to the corresponding acid. This was converted to the acid chloride **15** by treatment with oxalyl chloride. The synthesis of **16** has been previously described.[52] This was coupled with 0.2 equivalents of anthranoyl chloride to give the monosubstituted product **17**, which was coupled with 4-nitro-pyrrole-2-carbonyl chloride **15** to give **11**.

The isophthaloyl derivative **7** was synthesised by treating isophthaloyl dichloride with a large excess of pentafluoroaniline over 6 days (Scheme 7). Compound **7** was scarcely soluble in $CDCl_3$. Compound **11** has a solubility of about 0.5 mM in

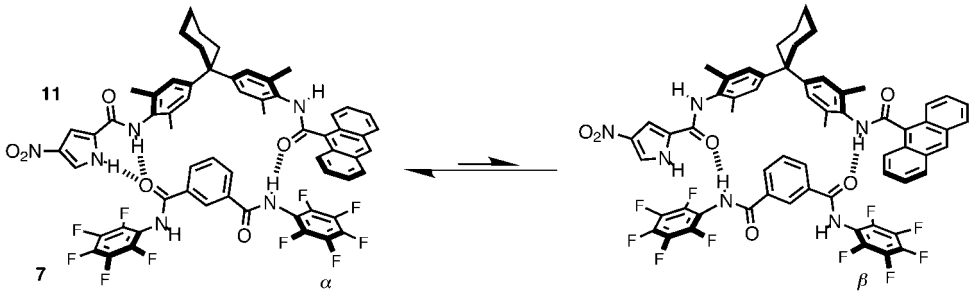

Scheme 5. Two possible conformations for complex **11**·**7**. The α geometry anthracene–aniline stacking interaction is favoured by the two bifurcated H-bonds formed by the nitropyrrole amide.

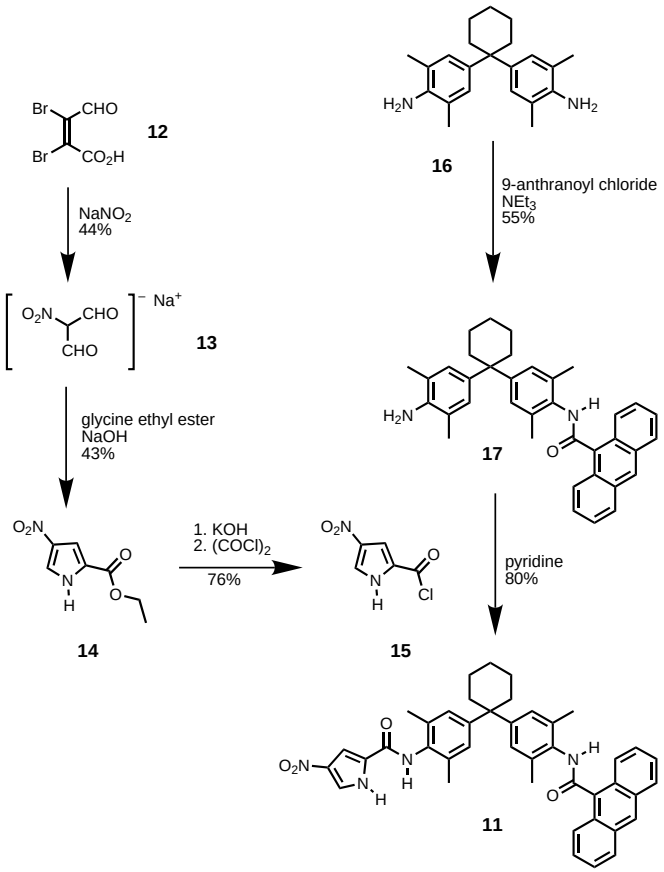

Scheme 6. Convergent synthesis of compound **11**.

$CDCl_3$, and even then precipitates after being in solution for 1–2 h. Thus complex **11·7** proved unsuitable for NMR titration experiments, and more soluble analogues were required.

A new target complex **18·6** was therefore designed (Scheme 8). A solubilising group **21** was added to the cyclohexyl ring of **11** and the pentafluoroaniline in **7** was replaced by 2,6-dimethylaniline. The X-ray structure analogues suggest that the aniline *ortho* methyl groups will keep

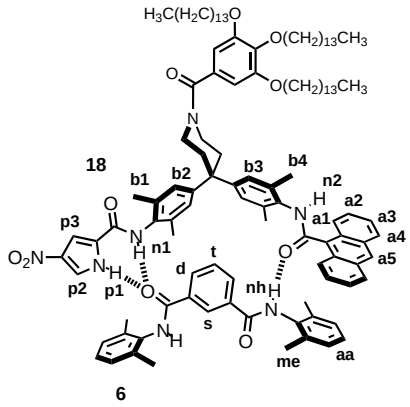

Scheme 8. Redesigned complex **18·6** for measuring aromatic stacking interactions. The proton labelling scheme is shown.

the rings in a stacked conformation, but the problems of the steric bulk associated with the isopropyl groups are almost eliminated. Schemes 9 and 10 show the relevant synthetic routes. Compound **21** was prepared from propyl gallate **19** according to Scheme 9. Compound **22** was prepared by heating 2,6-dimethylaniline and *N*-acetyl-4-piperidone in concentrated HCl under reflux. Protection of the aliphatic amine of **22** with benzylchloroformate in methanol gave **23**, which was then sequentially coupled with the anthracene and nitropyrrole acid chlorides. The protecting group was removed by using trimethylsilyl iodide according to a procedure described by Stammer.[53] The intermediate piperidine was extremely insoluble and was used without purification in a carbodiimide coupling with **21** to give the desired product **18**. The isophthaloyl derivative **6** has previously been described, but the synthesis is outlined in Scheme 7.[46]

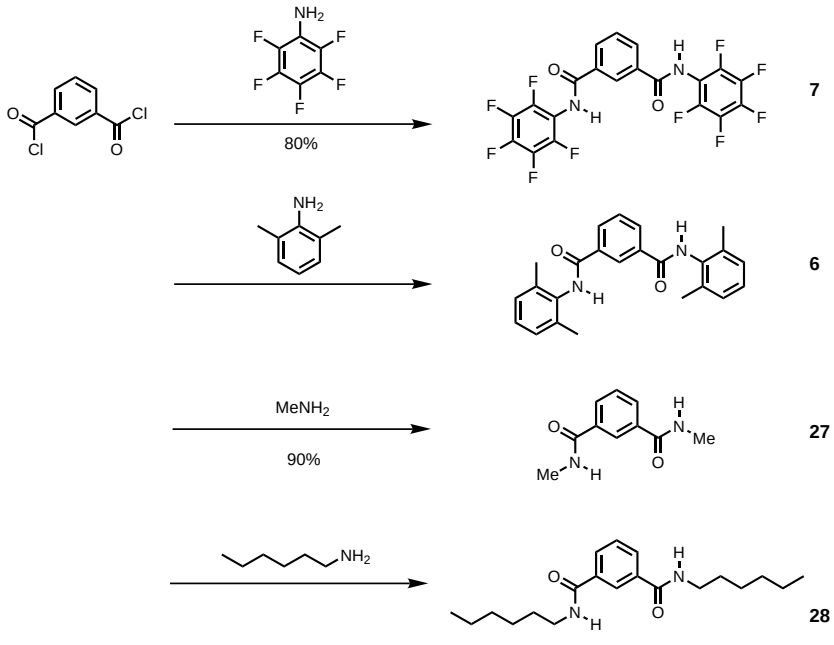

Scheme 7. Synthesis of compounds **6**, **7**, **27** and **28**.

Binding studies: ^{1}H NMR dilution experiments indicate that **6** has a dimerisation constant $K_d \approx 1\,\text{M}^{-1}$, but since **6** was used as the host at millimolar concentrations in the ^{1}H NMR titration experiments, the effects of dimerisation are negligible.[46] However, **18** was used as the guest at much higher concentrations, and ^{1}H NMR dilution experiments with **18** showed very large changes in chemical shift. The dilution data were fitted to both a dimerisation model and an aggrega-

0947-6539/01/0722-4866 $ 17.50+.50/0 *Chem. Eur. J.* **2001**, *7*, No. 22

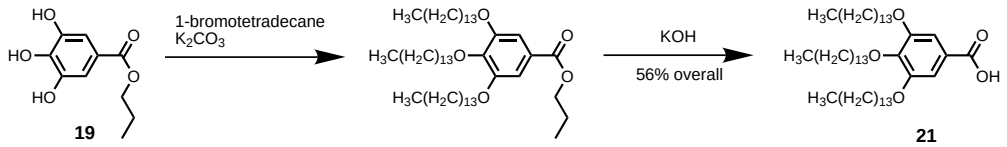

Scheme 9. Synthesis of compound **21** from **19**.

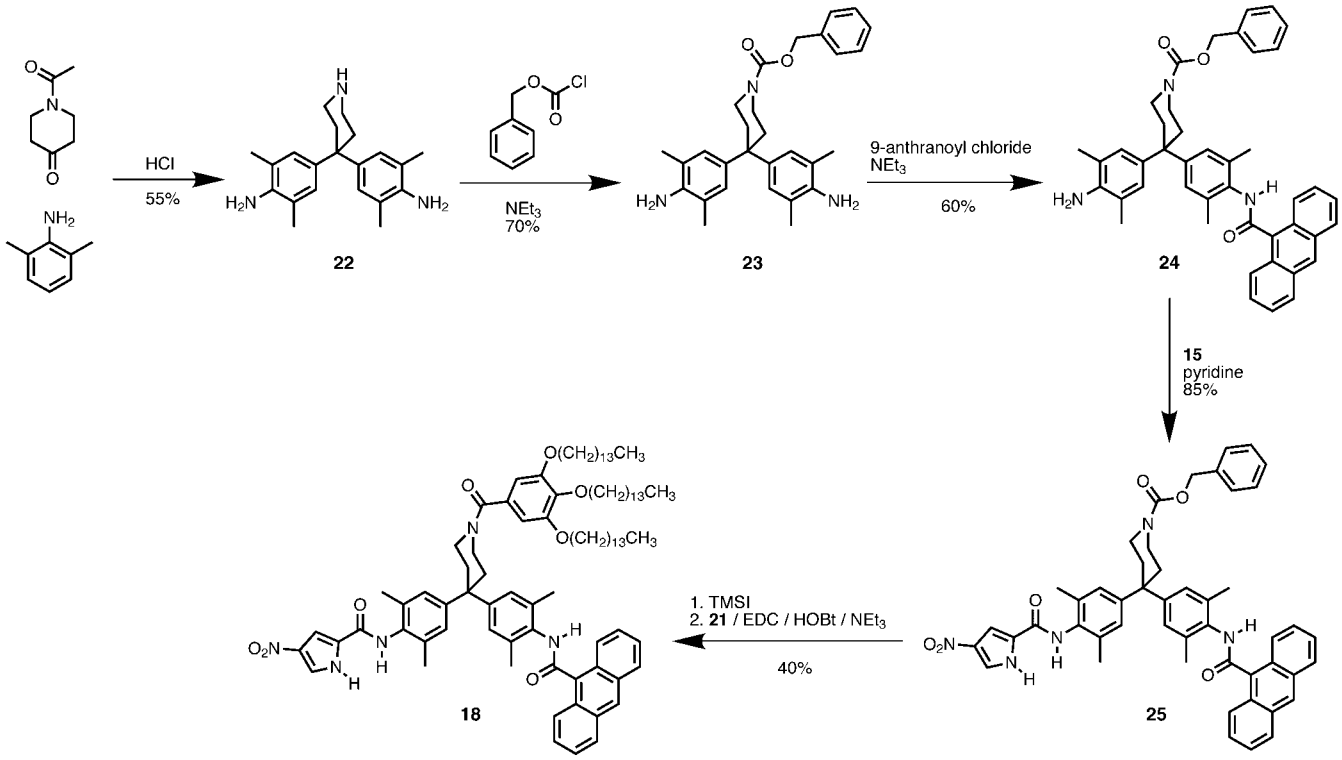

Scheme 10. Synthesis of compound **18**.

Table 1. Dimerisation constants K_d [M^{-1}] and limiting dimerisation-induced changes in chemical shift (ppm) for compounds **18**, **26** and **33** in $CDCl_3$ at 300 K.[a]

									Signal							
Compound	K_d	**p1**	**p2**	**p3**	**n1**	**n2**	**b1**	**b2**	**b3**	**b4**	**a1**	**a2**	**a3**	**a4**	**a5**	**m1**
18	13 ± 2	3.0	− 1.1	0.1	2.4	0.5	− 0.4	0.3	− 0.1	− 0.2	− 0.3	− 0.2	− 0.2	− 0.2	− 0.3	–
26	20 ± 2	2.9	− 0.7	nd[b]	2.0	1.1	nd[b]	0.1	− 0.1	− 0.2	–	–	–	–	–	− 0.1
33	11 ± 2	6.5	− 1.1	nd[b]	2.7	1.7	− 0.2	− 0.1	− 0.1	− 0.2	–	–	–	–	–	–

[a] See Schemes 8, 11 and 12 for proton labelling schemes. [b] Not determined due to signal overlap throughout the experiment. There are no significant changes in chemical shift for the signals due to the protons on the piperidine ring and solubilising group. Dilution experiments were repeated at least twice and K_d is the weighted mean based on the observed change in chemical shift for all the signals monitored. The error is twice the standard error.

tion model, but there is little difference in the results because at the concentrations of interest, the extent of interaction is small. The maximum percentage bound is 30%; this means that even if aggregation is the mode of association, the predominant species is dimer. From the dimerisation model, $K_d = 13 \pm 2\,M^{-1}$ for **18**. The limiting dimerisation-induced changes in chemical shift ($\Delta\delta$) are shown in Table 1. The magnitudes of the $\Delta\delta$ values imply that the main site of dimerisation is the nitropyrrole moiety. The $\Delta\delta$ values suggest that a bifurcated hydrogen bond is present, because there are large downfield shifts for the pyrrole and pyrrole amide NHs (Scheme 11a). In contrast, the X-ray crystal structure of the precursor **25** shows a different conformation for the nitro-

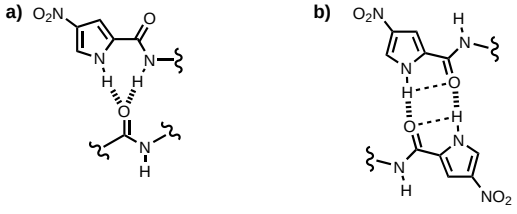

Scheme 11. a) The complexation-induced changes in ^1H NMR chemical shift indicate that the bifurcated H-bond motif is the principle mode of dimerisation for **18** in $CDCl_3$ solution. This stabilises the conformation in which the pyrrole NH is *anti* to the amide carbonyl oxygen. b) The H-bonding motif observed in the X-ray crystal structure of **25**. The conformation in which the pyrrole NH is *syn* to the carbonyl oxygen is stabilised by intramolecular H-bonding interactions.

pyrrole (Figure 1): the pyrrole NH is oriented *cis* to the amide carbonyl oxygen, and dimerisation occurs through two intermolecular pyrrole NH-amide H-bonds (Scheme 11b and Figure 1). This is almost certainly the lowest energy conformation of the nitropyrrole amide moiety in the monomer, because of intramolecular interactions between the

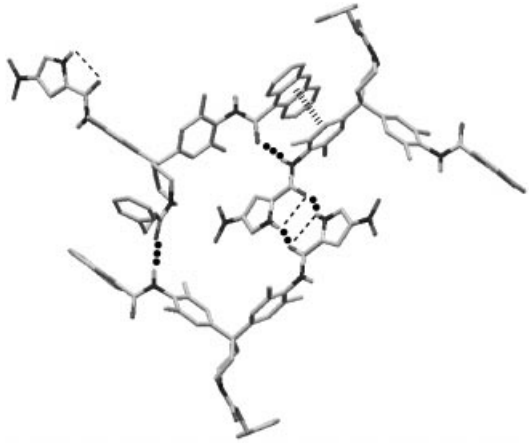

Figure 1. Three molecules from the X-ray crystal structure of **25**. The intermolecular stacking interaction between the anthracene and aniline is highlighted. The dashed lines denote intramolecular H-bonds, and the dotted lines denote intermolecular H-bonds.

pyrrole NH and amide carbonyl oxygen. In the solution dimer, however, it appears that the high energy conformation, that is when the pyrrole NH is *anti* relative to the amide carbonyl oxygen, is stabilised by the bifurcated H-bonding motif in Scheme 11a relative to the *syn* conformation. It is encouraging to note that in the crystal structure of **25** there is also an anthracene–aniline stacking interaction in precisely the arrangement we have designed into the **18·6** complex (Figure 1).

The ^{1}H NMR spectrum of **18** in deuterochloroform solution is further complicated by the fact that we can detect approximately 10% of a second conformer that is in slow exchange with the major species. The second conformer differs in the chemical shifts of the signals due to **p1** and **p3**, which appear at $\delta = 10.5$ and 5.3, respectively, as compared with $\delta = 10.7$ and 7.3 in the major conformer. These signals were readily assigned based on chemical exchange cross-peaks observed in a ROESY experiment. The rest of the ^{1}H NMR spectrum does not appear to be affected by the conformational change, and no other exchange cross-peaks were observed. The minor conformer disappears in [D$_6$]DMSO, either due to an increase in the rate of exchange or a decrease in the stability of the minor conformer. The large upfield shift observed for **p3** suggests that it sits over the face of an aromatic ring in the minor conformer, and the *syn-cis* conformation shown in Scheme 12 is the most likely explanation. The edge-to-face interaction involving the very polar **p3** proton presumably compensates for the energy required to isomerise the amide bond.

Thus there are four possible conformations for the pyrrole amide moiety, which are illustrated in Scheme 12. The conformers differ in the geometry of the amide bond (*cis* or *trans*)

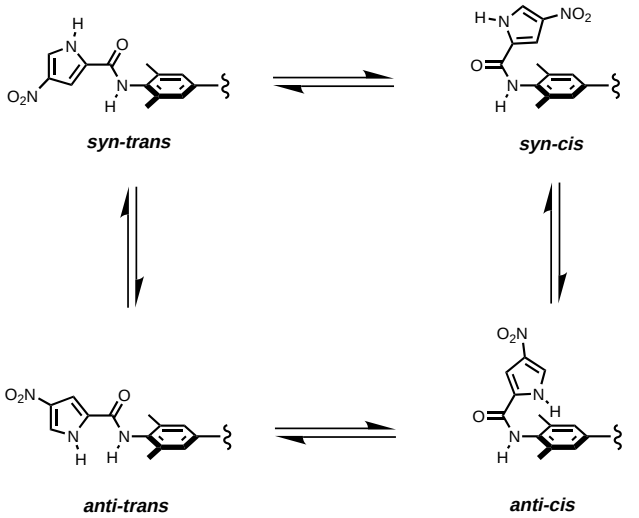

Scheme 12. Four possible conformations for the nitropyrrole amide moiety. The amide group can be *cis* or *trans*, and the pyrrole NH can be *syn* or *anti* with respect to the carbonyl oxygen.

and the arrangement of the pyrrole NH relative to the amide carbonyl group (*syn* or *anti*). The *syn-trans* conformation is probably the most stable and is the conformation found in the X-ray crystal structure of **25** (Figure 1). The *anti-trans* conformation appears to be the predominant species involved in dimerisation in solution. The *syn-cis* conformation is the second minor conformer observed in the ^{1}H NMR spectrum (molecular-mechanics calculations suggest that this is actually the lowest energy conformer). Exchange between *syn* and *anti* is fast on the NMR timescale, whereas exchange between *cis* and *trans* is slow, so it is not possible to rule out the presence of the *anti-cis* conformer, but the chemical shifts of the minor conformer suggest the *syn-cis* conformer is significantly more populated (**p3** is highly shielded and **p1** is not). In the dilution experiment, the ratio of the *cis* and *trans* conformers does not change significantly, but the extent of dimerisation is probably not enough to perturb the equilibrium. The signals due to **p1** and **p3** were not used in the determination of K_d for **18**, so the value measured in the dilution experiment is a weighted average for all the species present.

The binding constant of the **6·18** complex was determined by ^{1}H NMR titration experiments. Compound **18** was titrated into **6**, and the host signals were fitted to a 1:1 binding isotherm ($K_a = 85 \pm 7\,\text{M}^{-1}$). The data were also fitted to a model that allowed for dimerisation of the guest, and this gave a binding constant $K_a = 63 \pm 6\,\text{M}^{-1}$. Thus dimerisation of the guest makes a detectable difference in the titration results, and the significance of this in the double-mutant-cycle analysis will be discussed later. The limiting complexation-induced changes in chemical shift for formation of the **6·18** complex are shown in Figure 2 and Table 3. There are large downfield shifts of the signals due to the pyrrole NH and the pyrrole amide (**p1** and **n1**) as well as for the signal due to the amide of **6** (**nh**); these are indicative of H-bonding interactions. The change in chemical shift for the signal due to the anthracene amide (**n2**) is much smaller; this suggests that it is not H-bonded. The large upfield shift for the signal due to **p2**

0947-6539/01/0722-4868 $ 17.50+.50/0 *Chem. Eur. J.* **2001**, *7*, No. 22

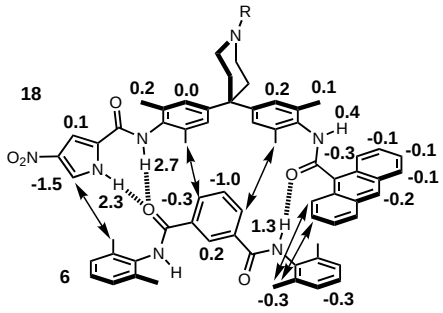

Figure 2. Limiting ^{1}H NMR complexation-induced changes in chemical shift (ppm) and intermolecular NOEs observed for complex **6·18** in $CDCl_3$ at 300 K.

of the pyrrole indicates that it sits over the face of an aromatic ring, so the complex clearly adopts the conformation shown in Figure 2 with **18** in the *anti-trans* conformation. The large upfield shift observed for the isophthaloyl triplet (**t**) and doublet (**d**) indicate that these protons lie over the face of another aromatic ring. The small downfield shifts observed for the signals due to the diarylmethane subunit (**b1**–**b4**) indicate that the face of this ring interacts with the edge of another and confirm that the expected edge-to-face interactions are present in the core of the complex.[54] Finally, the upfield shifts observed for all of the signals due to the anthracene of **18** and the aniline groups of **6** indicate that they are involved in a face-to-face stacking interaction. Five intermolecular NOEs were observed (Figure 2 and Table 2). The two **b**–**d** NOEs confirm that the isophthaloyl group is docked into the

Table 2. Intermolecular NOEs observed in two-dimensional ROESY experiments.[a]

Isophthaloyl compound	Bisaniline compound		
	18	**28**	**33**
6	**p2-me**, **b1-d**, **b4-d**, **a1-me**, **a2-me**	**b1-d**	**b1-d**, **b4-d**
28	**b1-d**, **b4-d**, **a1-nh**	**b1-d**, **b4-d**	**b1-d**, **b4-d**

[a] Experiments were carried out on 1:1 mixtures of the two components at the maximum concentration possible (3–28 mM). See Schemes 7, 8, 15 and 19 for the proton labelling schemes.

bisaniline pocket in the core of the complex. The remaining NOEs confirm that the nitropyrrole and anthracene both lie over the aniline rings of **6**.

In order to determine the effect of the minor conformer on the titration results, two titrations were carried out with **18** and the more soluble isophthaloyl compound **28**. In one titration **28** was the host and in the other it was the guest. With **28** as the host, $K_a = 49 \pm 8\,M^{-1}$. With **18** as the host, the signals for both the major and minor conformer could be followed throughout the titration and separately fitted to a binding isotherm that allowed for dimerisation of the host, but ignored the fact that the proportions of *cis* and *trans* conformers change during the titration. However, the guest was always present in a very large excess, and so this approximation does not affect the analysis. For the major *trans* conformer $K_{trans} = 70\,M^{-1}$ and for the minor *cis* conformer $K_{cis} = 12\,M^{-1}$. At the beginning of the experiment, the proportion of the *cis* conformer is approximately 10%, and the intensity of these signals decreases during the titration until they are barely detectable at the end. The results are summarised in Scheme 13.

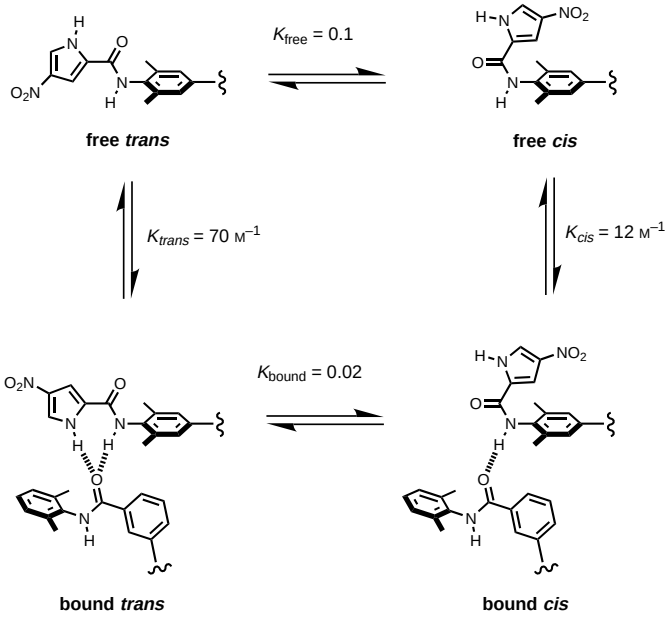

Scheme 13. Summary of conformational equilibria for **18** and the complex **28·18**. K_{free} is the *cis-trans* equilibrium constant for uncomplexed **18**. K_{trans} is the binding constant for the *trans* conformer of **18** with **28**. K_{cis} is the binding constant for the *cis* conformer of **18** with **28**. K_{bound} is the equilibrium constant for the *cis-trans* isomerism in the complex **18·28**.

Integration of the two sets of signals in the ^{1}H NMR spectrum of uncomplexed **18** gives the *cis-trans* equilibrium constant $K_{free} = 0.1$ (the *cis*/*trans* ratio) and, using this value with the two binding constants, we can calculate the *cis-trans* equilibrium constant in the **18·28** complex, $K_{bound} = 0.02$ (*cis*/*trans* ratio). Thus in the complex, the *trans* conformer is fifty times more stable than the *cis* conformer, and, because equilibration is fast on the timescale of the titration, the *cis* conformer cannot be observed at the end of the titration when saturation is reached. When **28** is the host, what we actually measure is the weighted average of the K_{trans} and K_{cis} equilibrium constants. The *cis-trans* ratio does not change in this experiment because **18** is always present in a large excess. Thus, using the results in Scheme 13, we can predict an expected value for the binding constant in the reverse titration:

$$K_a = (70 \times 0.9) + (12 \times 0.1) = 63\,M^{-1}$$

This explains why the association constant obtained from the reverse titration is lower. The predicted value is based on only one signal and, given the size of the errors involved, it is in reasonable agreement with the value measured experimentally, $K_a = 49 \pm 8\,M^{-1}$.

Double-mutant cycles: Despite the conformational complexity of uncomplexed **18**, these experiments show that this molecule is suitable for use in a double-mutant cycle to

measure the terminal aromatic stacking interaction. The complex adopts a single well-defined geometry, and the nitropyrrole provides a good β conformational lock forcing the α conformation required for aromatic stacking interactions at the other end of the complex. The nitropyrrole component is present in all four complexes in the double-mutant cycle, and so the thermodynamic consequences of the conformational equilibria in the uncomplexed state discussed above will cancel out in the analysis. In principle, the magnitude of the terminal aromatic interaction in complex A (**6·18**) in Scheme 14 can be estimated by chemical mutations which remove it: by comparing the stability of complex A with complexes B or C, which do not have the interaction present. However, this assumes that the aromatic rings in question make no other intermolecular interactions in complex A and that the strength of the hydrogen bonds remains constant when the aromatic to alkyl mutation is made. These effects are quantified by using the double mutant, complex D. For example, if we compare complexes C and D, the difference $\Delta G_C - \Delta G_D$ is a direct measure of the sum of the change in hydrogen bond strength and secondary interactions made by the anthracene group between complexes A and C. Thus the free energy difference of the two horizontal mutations in Scheme 14 allows us to dissect the interaction of interest from the complicated array of weak interactions present in complex A.

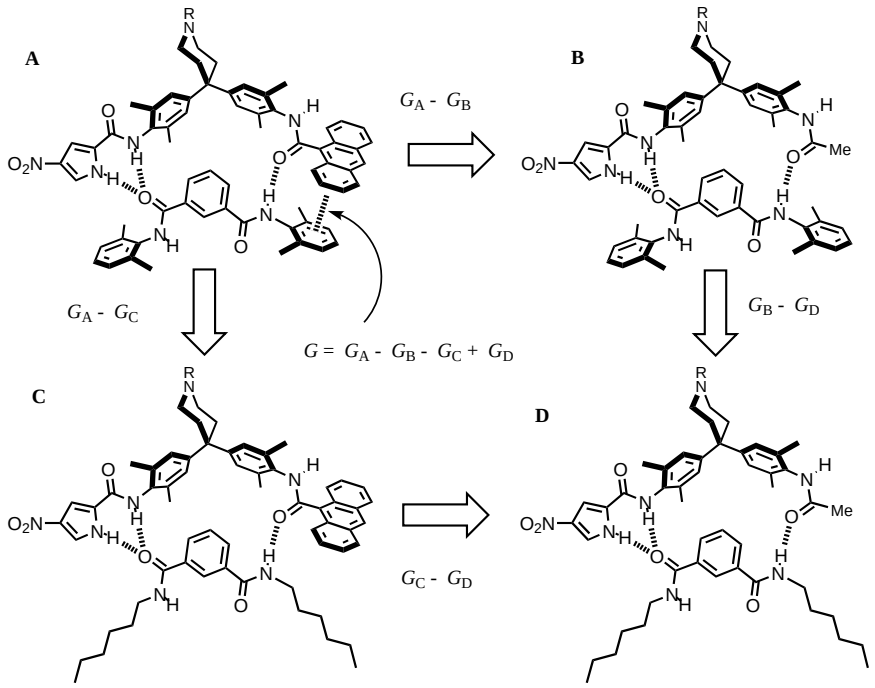

Scheme 14. Chemical double-mutant cycle to measure the anthracene–aniline stacking interaction in complex A (R = solubilising group, see Scheme 9).

The *N*,*N*′-dimethylisophthaloyl diamide **27** was synthesised according to Scheme 7 but was unsuitable for these experiments due to its low solubility, so the dihexyl derivative **28** was used instead. The synthesis of **28** has been described previously and is also outlined in Scheme 7.[46] The synthesis of **26** was carried out according to Scheme 15. Compound **23** was coupled with 4-nitropyrrole-2-carbonyl chloride (**15**). The

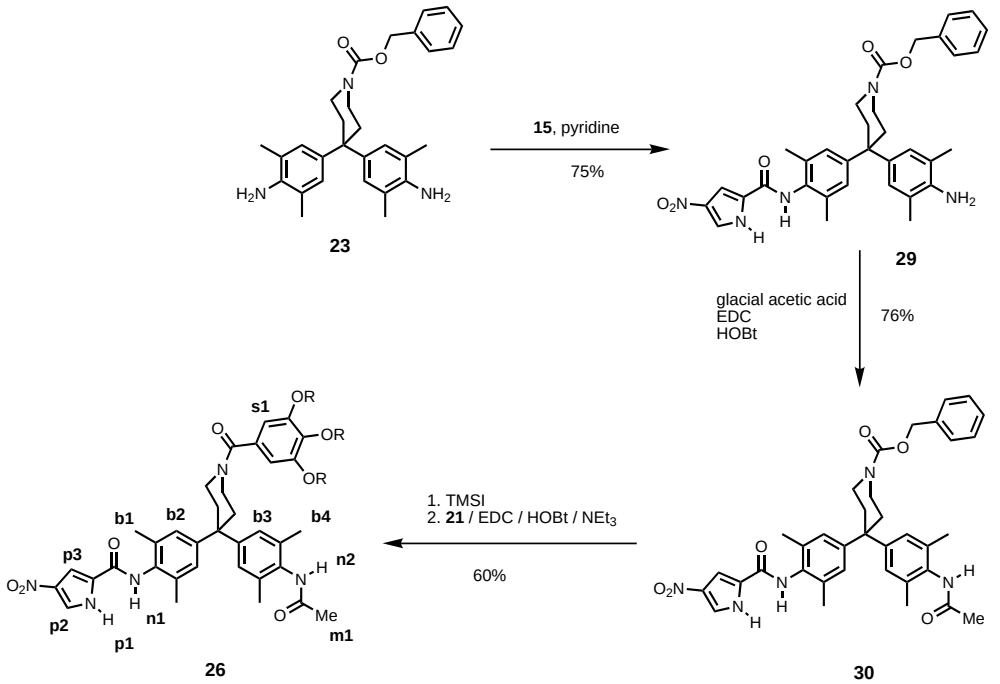

Scheme 15. Synthesis of compound **26** from **23**.

0947-6539/01/0722-4870 $ 17.50+.50/0 *Chem. Eur. J.* **2001**, *7*, No. 22

acetyl group was added by a carbodiimide coupling reaction. The product **30** was treated with TMSI to remove the protecting group and then reacted with **21** by a carbodiimide coupling to yield **26** in reasonable yield.

The dimerisation constant for **26** was determined by a ^{1}H NMR dilution experiment ($K_d = 20 \pm 2\,\text{M}^{-1}$). The limiting dimerisation-induced changes in chemical shift are shown in Table 1. The results are very similar to those obtained for **18**. The largest changes in chemical shift are associated with the pyrrole NH (**p1**) and the pyrrole amide (**n1**); this suggests the same mode of dimerisation in solution: the bifurcated H-bond motif shown in Scheme 11a. An X-ray crystal structure of the cyclohexyl analogue **31** (Figure 3), which was synthesised according to Scheme 16, shows that dimerisation in the solid state again occurs through a doubly H-bonded dimer of the pyrrole (cf Scheme 11b and Figure 1).

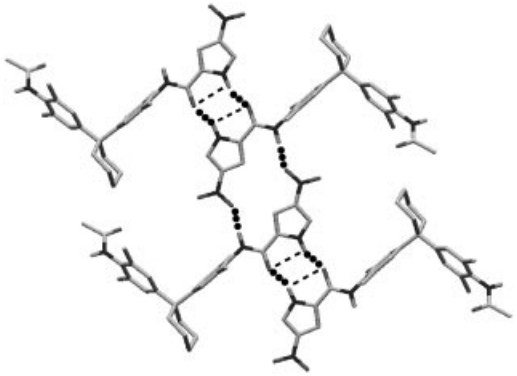

Figure 3. Three molecules from the X-ray crystal structure of **31**. The dashed lines denote intramolecular H-bonds, and the dotted lines denote intermolecular H-bonds.

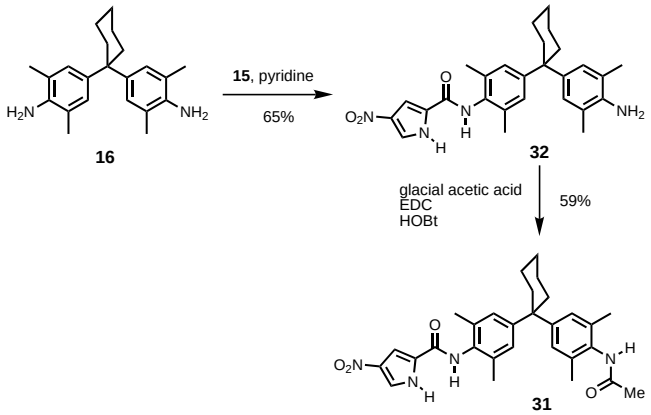

Scheme 16. Synthesis of compound **31** from **16**.

For **26** in $CDCl_3$, there are three different signals due to **p1** in the ^{1}H NMR spectrum, these collapse to one signal in DMSO. ROESY experiments show that all three **p1** signals are in chemical exchange, so it appears that there are three conformers of **26** in $CDCl_3$. **p3** shows a second minor signal at $\delta = 5.5$, which we attribute to the *syn-cis* geometry of the pyrrole subunit (Scheme 12), and the population of this conformer is 10% as observed previously for **18**. The new third conformer is more highly populated (20%) and is associated with a second signal due to **n2** in the ^{1}H NMR spectrum. The **n2** signal also collapses to one signal in DMSO, so we attribute the third conformer to the *cis* form of the acetamide. This conformational equilibrium does not affect any other signals in the spectrum, although it is surprising that it has an effect on **p1**. The conformer with both amides *cis* cannot be detected, but it must only be present at a level of about 2%.

In order to determine the effect of these minor conformers, two titrations were carried out with **26** and **28**, one in which **28** was the host and one in which it was the guest. With **28** as the host, $K_a = 46 \pm 6\,\text{M}^{-1}$. With **26** as the host, the signals for all three conformers could be followed and separately fitted to a binding isotherm that allowed for dimerisation of the host, again ignoring the changes in the populations of the three conformers, since the guest is present in a large excess. For the major *trans* conformer **p1** $K_{trans} = 64\,\text{M}^{-1}$, for the pyrrole *cis* conformer $K_{cis\text{-Pyr}} = 14\,\text{M}^{-1}$ and for the acetamide *cis* conformer $K_{cis\text{-Me}} = 6\,\text{M}^{-1}$. At the beginning of the experiment, the proportion of the pyrrole *cis* conformer is 10% and the proportion of acetamide *cis* conformer is 20%, but both decrease during the titration and cannot be detected at the end of the experiment. The results are summarised in Scheme 17.

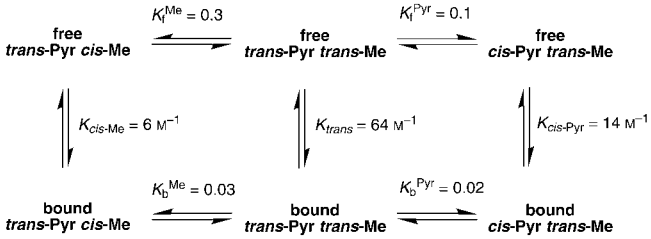

Scheme 17. Summary of conformational equilibria for **26** and the complex **28**·**26**. K_f^{Pyr} is the pyrrole amide *cis-trans* equilibrium constant. K_f^{Me} is the acetamide *cis-trans* equilibrium constant. K_{trans} is the binding constant for the all *trans* conformer of **26** with **28**. $K_{cis\text{-Pyr}}$ is the binding constant for the pyrrole amide *cis* conformer of **26** with **28**. $K_{cis\text{-Me}}$ is the binding constant for the acetamide *cis* conformer of **26** with **28**. K_b^{Pyr} is the equilibrium constant for the pyrrole amide *cis-trans* equilibrium in the complex **26**·**28**. K_b^{Me} is the equilibrium constant for the acetamide *cis-trans* equilibrium in the complex **26**·**28**.

From the pyrrole and acetamide *cis-trans* equilibrium constants for uncomplexed **26** and the three binding constants, we can calculate the *cis-trans* equilibrium constants in the **28**·**26** complex ($K_b^{Pyr} = 0.02$ and $K_b^{Me} = 0.03$). This means that the *trans* conformer is substantially stabilised in the complex, and the results for the pyrrole end of the complex are identical to those obtained for compound **18**. When **28** is the host, we actually measure the weighted average of K_{trans}, $K_{cis\text{-Pyr}}$ and $K_{cis\text{-Me}}$ equilibrium constants. Thus, using the results in Scheme 17, we can predict the value of the binding constant in the reverse titration:

$$K_a = (6 \times 0.2) + (64 \times 0.7) + (14 \times 0.1) = 47\,\text{M}^{-1}$$

This value is based on only one signal from each conformer but is in excellent agreement with the value measured experimentally, $K_a = 46 \pm 6\,\text{M}^{-1}$.

The implications of these equilibria for the double-mutant cycle must now be considered. In all the double-mutant cycle titrations, the bisaniline compound was used as the guest. Since several signals can be followed and they all behave in the same way, this avoids the complications of following signals from different conformations and allows a more accurate determination of the weighted-average binding constant for all of the conformers. The binding constants measured in this way are:

$$\text{for } \mathbf{18} \qquad K_{obs} = 0.1\,K_{cis} + 0.9\,K_{trans} \tag{1}$$

$$\text{for } \mathbf{26} \qquad K_{obs} = 0.1\,K_{cis\text{-Pyr}} + 0.2\,K_{cis\text{-Me}} + 0.7\,K_{trans} \tag{2}$$

Since K_{trans} is more than five times larger than the other binding constants, and the errors in the measurements are about 10%:

$$\text{for } \mathbf{18} \qquad K_{obs} \approx 0.9\,K_{trans} \tag{3}$$

$$\text{for } \mathbf{26} \qquad K_{obs} \approx 0.7\,K_{trans} \tag{4}$$

In the case of **26**, K_{trans} is $64\,\text{M}^{-1}$ and Equation (4) gives $K_{obs} \approx 45\,\text{M}^{-1}$, which is very close to the true weighted average of $47\,\text{M}^{-1}$. Ideally, we would like to construct double-mutant cycles using association constants for a single well-defined conformer, the *trans* conformer. However, using Equations (3) and (4), we can show that this is not required.

$$\begin{aligned}
\Delta\Delta G &= -\text{R}T\text{Ln}\left\{\frac{K_A\,K_D}{K_B\,K_C}\right\} \\
&= -\text{R}T\text{Ln}\left\{\frac{K_{trans}(\mathbf{6}\cdot\mathbf{18})\,K_{trans}(\mathbf{28}\cdot\mathbf{26})}{K_{trans}(\mathbf{6}\cdot\mathbf{26})\,K_{trans}(\mathbf{28}\cdot\mathbf{18})}\right\} \\
&= -\text{R}T\text{Ln}\left\{\frac{0.9\,K_{trans}(\mathbf{6}\cdot\mathbf{18}) \times 0.7\,K_{trans}(\mathbf{28}\cdot\mathbf{26})}{0.7\,K_{trans}(\mathbf{6}\cdot\mathbf{26}) \times 0.9\,K_{trans}(\mathbf{28}\cdot\mathbf{18})}\right\} \\
&\approx -\text{R}T\text{Ln}\left\{\frac{K_{obs}(\mathbf{6}\cdot\mathbf{18})\,K_{obs}(\mathbf{28}\cdot\mathbf{26})}{K_{obs}(\mathbf{6}\cdot\mathbf{26})\,K_{obs}(\mathbf{28}\cdot\mathbf{18})}\right\}
\end{aligned} \tag{5}$$

Although the absolute values of the observed binding constants are clearly affected by the mixture of conformers, in the double-mutant cycles, it is only the relative values of K_{trans} we are interested in. In other words, the weakly binding minor conformers do not affect the results of the double-mutant cycles, and we can use the observed binding constants, which are the weighted average of all species present. ^{1}H NMR titrations were carried out for all four complexes in the double-mutant cycle shown in Scheme 14, and the data were fitted to a simple 1:1 binding isotherm as well as a model that allows for dimerisation of the guest (Table 3). Although the two models gave quite different association constants, the overall $\Delta\Delta G$ values are similar: $+0.6 \pm 0.8\,\text{kJ mol}^{-1}$ for the 1:1 model and $+0.5 \pm 0.7\,\text{kJ mol}^{-1}$ for the 1:1 + dimerisation model. The reason is that the effects of dimerisation cancel out in the cycle in the same way as the effects of the conformational equilibria. Thus the double-mutant cycle provides a robust method for removing systematic errors from the titration measurements.

The limiting complexation-induced changes in chemical shift for all complexes are shown in Table 3. Although the magnitudes of the complexation-induced changes in chemical shift vary slightly, the pattern remains the same throughout the double-mutant cycle for all four complexes, so we can be confident that the structure of the core of the complex is not affected by the chemical mutations. The intermolecular NOEs detected in the two-dimensional ROESY spectra are shown in Table 2, and again the pattern of NOEs is consistent for all of the complexes. The stacking interaction measured for the anthracene – aniline system is slightly repulsive, but small. The result might be interpreted as the absence of any interaction between the two aromatic rings, since the value is zero within experimental error. However, the complexation-induced changes in chemical shift and NOEs show that the aromatic rings are stacked in close contact, and the measurement therefore represents a genuine evaluation of the stacking interaction rather than the absence of any interaction due to a problem with the geometry of the complex. The slightly repulsive interaction can be rationalised as the result of competition between favourable van der Waals interactions and repulsive electrostatic interactions between the π-electron systems.

As we have seen in the X-ray crystal-structure analysis of **10**, above, perfluorination of an aromatic ring makes aromatic-perfluoroaromatic stacking interactions favourable because the quadrupole moment is reversed in a fluorinated ring.[55] In order to quantify this effect by using our system, the double-

Table 3. K_a [M^{-1}] and ΔG [kJ mol^{-1}] values and limiting complexation-induced changes in chemical shifts (ppm) measured in $CDCl_3$ at 300 K for complexes used in the double-mutant cycles.[a]

Complex	1:1 Model		1:1 + Dimerisation Model		Isophthaloyl compound												Bisaniline compound			
	K_a	ΔG	K_a	ΔG	s	d	t	nh	aa	me	mu	p1	p2	p3	n1	n2	b1	b2	b3	b4
A																				
6·18	85 ± 7	−11.1 ± 0.2	63 ± 6	−10.3 ± 0.2	0.2	−0.3	−1.1	1.8	−0.3	−0.4	–	2.3	−1.5	0.1	2.7	0.4	0.2	0.0	0.2	0.1
6·33	168 ± 26	−12.8 ± 0.4	134 ± 22	−12.2 ± 0.4	0.1	−0.5	−1.2	1.3	−0.1	−0.2	–	2.3	−1.5	0.3	2.5	2.1	−0.1	0.1	−0.1	0.0
B																				
6·26	100 ± 23	−11.5 ± 0.6	73 ± 17	−10.7 ± 0.5	0.2	−0.4	−1.0	1.6	0.0	−0.1	–	2.1	−1.4	0.1	3.0	0.8	−0.1	0.2	−0.1	0.0
C																				
28·18	70 ± 9	−10.6 ± 0.3	49 ± 8	−9.7 ± 0.4	0.0	−0.4	−0.9	1.0	–	–	−0.5	2.3	−0.5	0.6	3.0	0.6	−0.2	−0.1	0.1	
28·33	102 ± 19	−11.5 ± 0.5	72 ± 16	−10.7 ± 0.6	0.0	−0.3	−0.5	0.6	–	–	−0.2	3.2	−0.4	0.4	2.3	1.9	−0.2	−0.2	−0.3	−0.1
D																				
28·26	65 ± 6	−10.4 ± 0.3	46 ± 6	−9.5 ± 0.3	0.1	−0.4	−0.8	1.0	–	–	−0.1	2.5	−0.5	0.6	3.1	0.9	−0.2	−0.1	−0.1	−0.1

[a] See Schemes 7, 8, 15 and 19 for the proton labelling schemes. There are no significant changes in chemical shift for the signals due to the protons on the piperidine ring and solubilising group R. Titration experiments were repeated at least twice and K_a is a weighted mean based on the observed change in chemical shift for all the signals monitored. The error is twice the standard error.

0947-6539/01/0722-4872 $ 17.50+.50/0 *Chem. Eur. J.* **2001**, *7*, No. 22

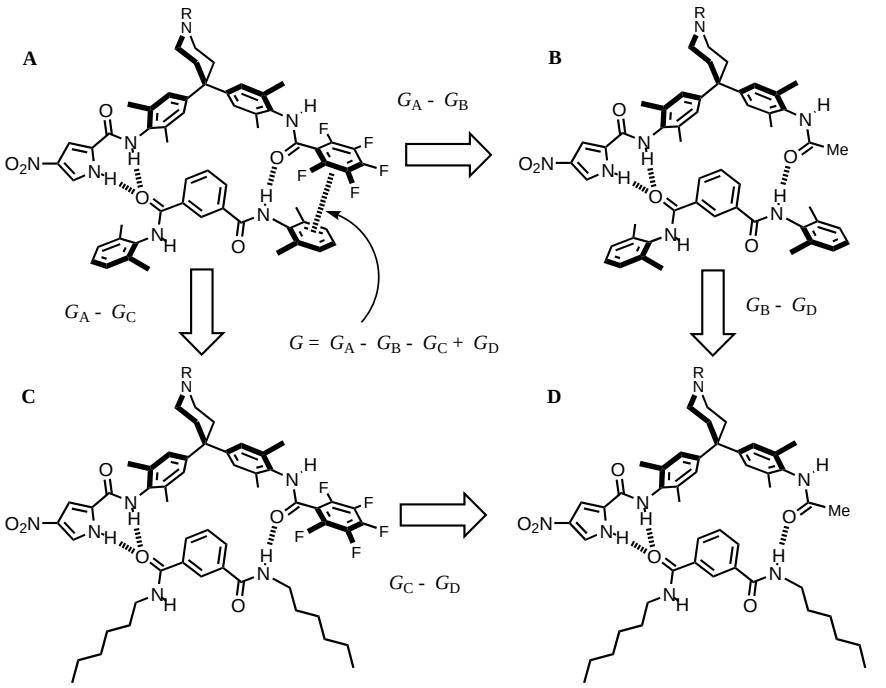

Scheme 18. Chemical double-mutant cycle to measure the pentafluorophenyl–aniline stacking interaction in complex A (R = solubilising group, see Scheme 9).

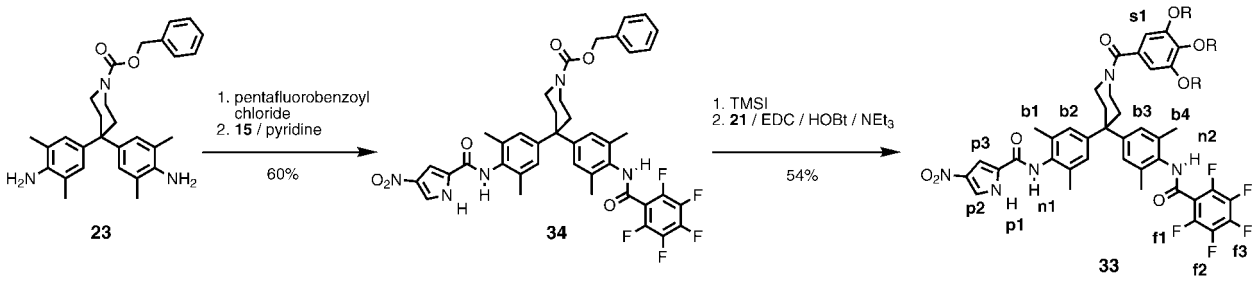

Scheme 19. Synthesis of compound **33** from **23**.

mutant cycle in Scheme 18 was designed. Compound **33** was prepared according to Scheme 19. The solubility of **33** is lower than the anthracene and methyl derivatives used previously (9 mM versus 50 mM), and this limits the accuracy of titration experiments with this system. A ^{1}H NMR dilution experiment gave $K_d = 11 \pm 2\,M^{-1}$, and the dimerisation-induced changes in chemical shift are shown in Table 1. As before, the main site of dimerisation is the pyrrole NH and pyrrole amide (Scheme 11a).

a1	a2	a3	a4	a5	m1
– 0.3	– 0.1	– 0.1	– 0.1	– 0.2	–
–	–	–	–	–	–
–	–	–	–	–	– 0.4
– 0.2	– 0.2	– 0.2	– 0.1	– 0.2	–
–	–	–	–	–	–
–	–	–	–	–	0.0

Compound **33** has minor conformers similar to those in **18**, but because we have shown that they have an insignificant effect on the overall result of the double-mutant cycle, they were ignored in this experiment. The results of ^{1}H NMR titrations and the complexation-induced changes in chemical shift for the complexes in the pentafluorophenyl double-mutant cycle are shown in Table 3. The pattern is similar to the anthracene–aniline experiment. The complexation-induced changes in chemical shift of the fluorine atoms were also determined. For complex **6**·**33**, the changes in chemical shift are: $\Delta\delta = -1.0$ ppm (**f1**), -0.3 ppm (**f2**) and -0.1 ppm (**f3**). For complex **28**·**33**, the changes in chemical shift are: $\Delta\delta = -0.1$ ppm (**f1**), -0.4 ppm (**f2**) and -0.2 ppm (**f3**). These were determined in the same way as the proton shifts, but it is difficult to interpret these changes. Using the results of the ^{1}H NMR titrations in a double-mutant cycle, we find that the pentafluorophenyl–aniline interaction is slightly attractive, $\Delta\Delta G = -0.4 \pm 0.9$ kJ mol^{-1}. Although this value is within experimental error of the anthracene–aniline interaction, the pentafluorophenyl–aniline interaction is more attractive, and this can be rationalised based on the change in the quadrupole moment of the π-system which leads to more favourable electrostatic interactions for the pentafluorophenyl interaction.

Conclusion

We have developed a system to measure aromatic stacking interactions in which we can dictate the geometry of the complexes by using a combination of noncovalent interactions. The system is capable of measuring both attractive and repulsive aromatic interactions while maintaining the same geometry throughout the experiments. The effects of dimerisation and other conformational equilibria have been taken into account, but have been shown to cancel out in the double-mutant cycle. X-ray crystallography is a powerful tool in the design of molecular complexes and reveals the geometry of aromatic interactions that can be expected in solution. This system has the potential to be used to probe other aromatic interactions by changing the size and electronic nature of the interacting rings to fully investigate structure-activity relationships in aromatic stacking.

Experimental Section

NMR Experiments: ^{1}H, ^{19}F and ^{13}C spectra were recorded on either a Bruker AC250 or AMX400 spectrometer with residual solvent as an internal standard. Fluorine chemical shifts were referenced to an external $CFCl_3$ reference. Two-dimensional ROESY experiments were recorded on a Bruker AMX2-400 with 300 ms mixing time and a 3 s relaxation delay between pulses.

For the ^{1}H NMR dilution experiments, a 2.0 mL sample of known concentration was prepared in $CDCl_3$. Aliquots of this solution were sequentially added to 0.5 mL of $CDCl_3$, and a ^{1}H NMR spectrum recorded after each addition. All dilutions were repeated twice. A two-dimensional ROESY experiment was carried out on the final solution to assign unambiguously all of the signals, and the data were analysed by using nonlinear curve fitting for both dimerisation and aggregation isotherms *NMRDil Dimer* and *NMRDil Agg*.[56] These estimate the dimerisation constant and the limiting bound and free chemical shifts. The dimerisation constant is quoted as the weighted mean based on the observed change in chemical shift for all of the signals monitored. The error is twice the standard error.

^{1}H NMR titrations were carried out by preparing a 3 mL sample of the host at known concentration (3–4 mM). 0.5 mL of this solution was removed, and a ^{1}H NMR spectrum was recorded. An accurately weighed sample of the guest was then dissolved in 2 mL of the host solution. The solution was saturated with guest (35–40 mM) to allow access to as much of the binding isotherm as possible (50–86 % was achieved) and contained host, so that the concentration of host remained constant during the titration. Aliquots of guest solution were added successively to the NMR tube containing the host solution, and the ^{1}H NMR spectrum was recorded after each addition. Signals that moved more than 0.01 ppm were analysed by using nonlinear curve fitting, *NMRTit HG* and *NMRTit HGHHGG*.[57] *NMRTit HG* fits the data to a 1:1 binding model to give the association constant and the limiting bound chemical shift in the complex, and *NMRTit HGHHGG* fits the data to a 1:1 binding isotherm, allowing for dimerisation of both binding partners. The association constant for each experiment was evaluated as the weighted mean based on the observed change in chemical shift for all signals monitored. The error was taken as twice the standard error.

Titrations where the identities of the host and guest could be reversed were used to determine the limiting complexation-induced shifts for both binding partners. However, this was not possible in cases where the solubility of the guest was not sufficient to achieve saturation. In these cases, a 1:1 mixture of the two components was prepared, and the ^{1}H NMR spectrum was recorded. A ROESY experiment was used to unambiguously assign all of the signals. By using the limiting complexation-induced changes in chemical shift for one of the components from the titration experiment ($\Delta\delta_{bound}$) and the free chemical shift from the dilution experiments, the proportion of bound complex could be determined:

$$\text{fraction bound} = \Delta\delta_{obs}/\Delta\delta_{bound} \quad (6)$$

The observed change in chemical shift of the other compound in the 1:1 mixture could then be used to determine the limiting complexation-induced changes in chemical shift ($\Delta\delta_{bound}$).

$$\Delta\delta_{bound} = \Delta\delta_{obs}/\text{fraction bound} \quad (7)$$

In order to verify this method, a titration was carried out with the identities of the host and guest reversed (**18**·**28**), and the signals were analysed with *NMRTit HG* (**18** was used at low concentration, so there should be an insignificant amount of dimerisation) to determine the limiting complexation-induced changes in chemical shift. The results are compared with the values obtained by the fraction bound method in Table 4. Except for the value for **p2**, reasonable agreement is obtained; this indicates that the method used to determine the limiting complexation-induced changes in chemical shift is reliable.

General synthetic procedures: The reactions were carried out according to the following general procedures unless otherwise stated.

Acid chloride preparation: Acid chlorides were formed by suspending the corresponding acid in dry CH_2Cl_2 under a nitrogen atmosphere. An excess of oxalyl chloride and 1–2 drops of catalytic DMF were added. The reaction mixture was stirred until all the acid had gone into solution (typically 0.5–1.0 h), and the CH_2Cl_2 and excess oxalyl chloride were removed under reduced pressure. The acid chloride was used without further purification.

Amide coupling reactions: These reactions were carried out in CH_2Cl_2 under a nitrogen atmosphere. The acid chloride was prepared as above, dissolved in CH_2Cl_2 and added drop-wise to a stirred solution of the amine and base (where applicable) in CH_2Cl_2 (50–200 mL). The reactions were stirred for 16 h and the solvent was then removed under reduced pressure. The product was isolated by column chromatography.

Piperidine deprotection and addition of the solubilising group: The benzylchloroformate-protected compound was dissolved in CH_2Cl_2. TMSI was added, and the mixture was stirred until the reaction was completed as determined by TLC (0.5–16 hours). The solvent was removed under reduced pressure, and the resulting solid was washed repeatedly with diethyl ether and dried. Compound **21**, 1-hydroxybenzotriazole (HOBt) and 1,3-(dimethylaminopropyl)-3-ethylcarbodiimide hydrochloride (EDC) were dissolved in CH_2Cl_2 and stirred for 1 h, and then the free piperidine was added portion-wise with a few drops of triethylamine. The reaction mixture was stirred for 16 h. The reaction was quenched with methanol (2 mL), and the solvent was removed under reduced pressure. The product was isolated by medium-pressure column chromatography (CH_2Cl_2/methanol 98:2). The product was dissolved in CH_2Cl_2, washed with 1M HCl, sat. Na_2HCO_3 and water and dried over Na_2SO_4. The solvent removed under reduced pressure.

***N*-[(2,6-Diisopropyl)phenyl]-9-anthracene carboxamide (8)**: Compound **8** was prepared by the standard amide coupling procedure by using 9-anthracene carboxylic acid (1.5 g, 6.76 mmol) in CH_2Cl_2 (40 mL), 2,6-diisopropyl aniline (1.0 g, 5.64 mmol) and triethylamine (0.57 g, 5.64 mmol) in CH_2Cl_2 (50 mL). Purification by column chromatography yielded a pale yellow solid. Yield: 0.9 g, 28 %; m.p. decomposes >206 °C; ^{1}H NMR (250 MHz, $CDCl_3$, 25 °C, TMS): $\delta = 8.54$ (s, 1H), 8.41 (d, $^3J(H,H) = 7$ Hz, 2H), 8.07 (d, $^3J(H,H) = 7$ Hz, 2H), 7.54 (m, 4H), 7.38 (t, 1H), 7.29 (m, 2H), 3.54 (sept, $^3J(H,H) = 7$ Hz, 2H), 2.14 (d, $^3J(H,H) = 7$ Hz, 12H); ^{13}C NMR

Table 4. Fraction bound calculations and limiting complexation-induced changes in chemical shift (ppm) for complex **28**·**18**.

	δ_{free}	$\delta_{mixture}$	$\Delta\delta_{obs}$	$\Delta\delta_{bound}$	% B	$\Delta\delta_{bound}$[a]	$\Delta\delta_{bound}$[b]
Host 28							
nh	6.292	6.616	0.324	0.77	42		
d	7.893	7.740	0.153	0.30	50		
mu	3.447	3.275	0.172	0.34	49		
Guest 18							
p1	9.85	10.35	0.50	–	–	2.3	1.3
p2	7.79	7.47	−0.32	–	–	−0.5	−0.04
p3	7.28	7.30	0.02	–	–	0.6	nd[c]
n1	7.14	7.71	0.57	–	–	3.0	2.2
n2	7.23	7.32	0.09	–	–	0.6	0.7
b1	2.25	2.21	0.04	–	–	−0.2	−0.1
b2	7.04	7.04	0.00	–	–	−0.1	0.0
b3	7.07	7.11	0.05	–	–	0.1	0.1
b4	5.52	2.53	0.01	–	–	−0.1	0.0
a1	8.35	8.29	−0.06	–	–	−0.2	−0.1
a2	7.55	7.53	−0.02	–	–	−0.2	nd
a3	7.55	7.53	−0.02	–	–	−0.2	nd
a4	8.07	8.04	−0.03	–	–	−0.1	−0.1
a5	8.55	8.50	−0.05	–	–	−0.2	−0.1

[a] $\Delta\delta_{bound}$ calculated by fraction bound method. [b] $\Delta\delta_{bound}$ determined by reverse titration method. [c] Not determined due to signal overlap during the experiment.

0947-6539/01/0722-4874 $ 17.50+.50/0 *Chem. Eur. J.* **2001**, *7*, No. 22

(250 MHz, $CDCl_3$, 25 °C): $\delta = 169.0, 146.2, 131.7, 131.2, 130.5, 128.8, 128.7, 128.5, 125.1, 123.8, 29.0, 24.0$; FAB MS: *m/z*: 381 $[M]^+$.

***N*-[(2,6-Dimethyl)phenyl]-9-anthracene carboxamide (9)**: Compound **9** was prepared by the standard amide coupling procedure with 9-anthracene carboxylic acid (2.2 g, 9.90 mmol) in CH_2Cl_2 (30 mL), 2,6-dimethylaniline (1.0 g, 8.25 mmol) and triethylamine (0.84 g, 8.25 mmol). Purification by column chromatography yielded a pale yellow solid. Yield: 1.0 g, 38 %; m.p. decomposes > 225 °C; ^{1}H NMR (250 MHz, $CDCl_3$, 25 °C, TMS): $\delta = 8.50$ (s, 1H), 8.37 (d, ^3J(H,H) = 9 Hz, 2H), 8.03 (d, ^3J(H,H) = 9 Hz, 2H), 7.65 – 7.45 (m, 4H), 7.3 (brs, 1H), 6.55 (brs, 2H), 2.50 (s, 6H); ^{13}C NMR (250 MHz, $CDCl_3$, 25 °C): $\delta = 168.0, 135.3, 133.8, 132.0, 131.3, 128.8, 128.5, 127.8, 127.0, 125.7, 125.3, 193.8$; FAB MS: *m/z*: 325 $[M]^+$.

***N*-Pentafluorophenyl-9-anthracene carboxamide (10)**: Compound **10** was prepared by the standard amide coupling procedure with 9-anthracene carboxylic acid (0.25 g, 1.13 mmol) in CH_2Cl_2 (30 mL), pentafluoroaniline (0.28 g, 1.24 mmol) and triethylamine (0.12 g, 1.24 mmol) in CH_2Cl_2 (50 mL). The reaction was stirred for 3 days. Purification by column chromatography yielded a pale yellow solid. Yield: 0.18 g, 40 %; m.p. decomposes > 220 °C; ^{1}H NMR (250 MHz, $CDCl_3$, 25 °C, TMS): $\delta = 8.5$ (s, 1H), 8.13 (d, ^3J(H,H) = 9 Hz, 2H), 8.04 (d, ^3J(H,H) = 9 Hz, 2H), 7.6 – 7.5 (m, 4H), 7.34 (brs, 1H); ^{13}C NMR (250 MHz, $CDCl_3$, 25 °C): $\delta = 134.1, 130.9, 129.3, 128.6, 128.1, 127.4, 125.7, 124.4$; ^{19}F NMR ($CDCl_3$) $\delta = -144, -156, -162$; FAB MS: *m/z*: 387 $[M]^+$.

***N*-(9-Anthranoylcarboxy)-{1,1-bis[(4-amino-3,5-dimethyl)phenyl]cyclohexane} (17)**: Compound **17** was prepared by the standard amide coupling procedure with 9-anthracene carboxylic acid (1.07 g, 4.8 mmol) in CH_2Cl_2 (50 mL), bisaniline **16** (7.74 g, 24.0 mmol) and triethylamine (0.48 g, 4.8 mmol). The reaction mixture was washed with 1M HCl to remove excess **16**. Purification by column chromatography gave a yellow solid. Yield: 1.34 g, 55 %; m.p. 175 – 178 °C; ^{1}H NMR (250 MHz, $CDCl_3$, 25 °C, TMS): $\delta = 8.50$ (s, 1H), 8.35 (d, ^3J(H,H) = 9 Hz), 8.02 (d, ^3J(H,H) = 7 Hz), 7.52 (m, 4H), 7.21 (s, 1H), 7.08 (s, 2H), 6.89 (s, 2H), 3.47 (brs, 2H), 2.47 (s, 6H), 3.44 (brm, 4H), 2.16 (s, 6H), 1.58 (brm, 6H); ^{13}C NMR (250 MHz, $CDCl_3$, 25 °C): $\delta = 167.8, 148.9, 140.0, 137.5, 134.4, 132.0, 131.1, 130.7, 128.6, 128.5, 128.3, 127.3, 127.0, 126.8, 125.5, 125.2, 121.5, 44.9, 37.2, 26.4, 23.0, 20.1, 18.1$; FAB MS: *m/z*: 526 $[M]^+$; elemental analysis calcd (%) for $C_{37}H_{38}N_2O \cdot 0.5\,H_2O$: C 82.95, H 7.33, N 5.22; found C 82.57, H 7.14, N 5.18.

***N*-(9-Anthranoylcarboxy)-*N*′-(4-nitropyrrole-2-carboxy){1,1-bis[(4-amino-3,5-dimethyl)phenyl]cyclohexane} (11)**: Compound **11** was prepared by the standard amide coupling procedure with 4-nitropyrrole-2-carboxylic acid (1.74 g, 11.2 mmol) in CH_2Cl_2 (30 mL), **17** (4.51 g, 8.57 mmol) and pyridine (1.35 g, 17.1 mmol). The reaction mixture was washed with 1M HCl and water. Purification by column chromatography gave a pale yellow solid. Yield: 4.5 g, 80 %; m.p. > 300 °C; ^{1}H NMR (250 MHz, [D$_6$]DMSO, 25 °C, TMS): $\delta = 12.93$ (s, 1H), 10.16 (s, 1H), 9.63 (s, 1H), 8.75 (s, 1H), 8.25 (d, ^3J(H,H) = 8 Hz, 2H), 8.19 (d, ^3J(H,H) = 8 Hz, 2H), 7.98 (s, 1H), 7.67 – 7.57 (m, 4H), 7.18 (s, 2H), 7.16 (s, 2H), 2.47 (s, 6H), 2.32 (brm, 4H), 2.18 (s, 6H), 1.52 (brm, 6H); ^{13}C NMR (250 MHz, [D$_6$]DMSO, 25 °C): $\delta = 168.6, 158.7, 147.8, 147.6, 137.2, 135.2, 134.8, 131.3, 131.1, 130.2, 128.6, 128.1, 127.4, 126.8, 125.6, 125.5, 124.8, 106.0, 45.2, 37.0, 31.1, 26.3, 22.9, 19.9, 18.6$; FAB MS: *m/z*: 665 $[M+H]^+$; elemental analysis calcd (%) for $C_{42}H_{40}N_4O_4 \cdot H_2O$: C 73.87, H 6.20, N 8.20; found C 74.13 H 6.03 N 8.20.

***N*,*N*′-Bis-pentafluorphenyl isophthaldiamide (7)**: Compound **7** was prepared by the standard amide coupling procedure with isophthaloyl dichloride (0.30 g, 1.5 mmol) and pentafluoroaniline (1.08 g, 5.9 mmol) in CH_2Cl_2 (50 mL). The reaction was stirred for 6 days, and a colourless precipitate formed. The reaction mixture was diluted with CH_2Cl_2, washed with 1M NaOH, 1M HCl and water and dried over Na_2SO_4. The solvent was then removed under reduced pressure. The product was recrystallised form ethanol/water to give a colourless solid. Yield: 0.59 g, 80 %; m.p. > 250 °C; ^{1}H NMR (250 MHz, [D$_6$]DMSO, 25 °C, TMS): $\delta = 10.83$ (brs, 2H), 8.63 (s, 1H), 8.26 (d, ^3J(H,H) = 8 Hz, 2H), 7.77 (t, 1H, ^3J(H,H) = 8 Hz); ^{19}F NMR ($CDCl_3$/CD_3OD) $\delta = -145, -153, -163$; FAB MS: *m/z*: 497 $[M+H]^+$; elemental analysis calcd (%) for $C_{20}H_6F_{10}N_2O_2 \cdot 0.5\,H_2O$: C 47.54, H 1.40, N 5.54; found C 47.84, H 1.32, N 5.54.

(3,4,5-Tri-*O*-tetradecane)benzoic acid (21): *n*-Propyl gallate **19** (5.55 g, 26.2 mmol), 1-bromodecane (22 mL, 78.6 mmol) and anhydrous K_2CO_3 (32.2 g, 236 mmol) were suspended in a mixture of acetone/DMSO (9:1, 100 mL). The mixture was stirred for 30 minutes and then heated under reflux for 10 h. The reaction mixture was poured into water (1500 mL), and the pH brought to about 5 by the addition of 10 % *v*/*v* formic acid. The product was extracted with CH_2Cl_2 and dried over Na_2SO_4. The solvent was removed under reduced pressure, and the resulting syrup was purified by column chromatography directly through basic alumina (CH_2Cl_2) to yield the intermediate ester **20**.

Compound **20** (26.2 mmol) was suspended in a solution of KOH (3.93 g, 66 mmol) in ethanol/water (19:1, 130 mL) and heated under reflux for 1 h. The reaction was cooled and brought to pH 5 with 10 % *v*/*v* formic acid. Compound **21** precipitated upon further cooling, it was recrystallised from hot ethanol (225 mL) before being dried in a vacuum oven to yield a colourless waxy solid. Yield: 11 g, 56 %; m.p. 43 – 45 °C; ^{1}H NMR (250 MHz, $CDCl_3$, 25 °C, TMS): $\delta = 7.31$ (s, 2H), 4.10 – 4.00 (m, 6H), 1.85 – 1.70, 1.50 – 1.20, 1.20 – 1.0 (brm, 72H), 0.90 – 0.80 (m, 6H); elemental analysis calcd (%) for $C_{50}H_{90}O_5$: C 77.87, H 11.76; found C 77.52, H 11.95.

[4,4-Bis(4-amino-3,5-dimethylphenyl)]piperidine (22): A mixture of 2,6-dimethylaniline (117 g, 1236 mmol), *N*-acetyl-4-piperidone (63.5 g, 449 mmol) and conc. HCl (150 mL) was heated under reflux. On the second day, 2,6-dimethylaniline (15 g, 120 mmol) was added to the refluxing mixture. This was repeated on the fourth day of reflux. After 6 days, the reaction mixture was cooled to room temperature and diluted with water (1200 mL). The reaction was neutralised by addition of solid sodium carbonate, and the resulting precipitate was filtered off and washed with water, diethyl ether and pentane. The resulting colourless powder was dried to give a colourless solid. Yield: 87.5 g, 60 %; m.p. 203 – 205 °C; ^{1}H NMR (250 MHz, [D$_6$]DMSO, 25 °C, TMS): $\delta = 8.85$ (brs, 1H), 6.71 (s, 4H), 4.41 (brs, 4H), 2.95 – 2.90 (brm, 4H), 2.45 – 2.40 (brm, 4H), 2.09 (s, 12H); ^{13}C NMR (250 MHz, [D$_6$]DMSO, 25 °C): $\delta = 141.9$, 134.9, 127.8, 120.6, 115.9, 41.4, 41.1, 32.8, 18.2; FAB MS: *m/z*: 324 $[M+H]^+$.

(1-Benzyloxycarbonyl)-[4,4-bis(4-amino-3,5-dimethylphenyl)]piperidine (23): Compound **22** (14.1 g, 44 mmol) and triethylamine (9.1 mL 66 mmol) were dissolved in methanol (250 mL). Benzylchloroformate (6.9 mL 48 mmol) in methanol (30 mL) was added dropwise. The reaction mixture was stirred for 16 h, and the reaction mixture was reduced to half the original volume under reduced pressure. Water (200 mL) was added, and the resulting precipitate was filtered and washed repeatedly with petroleum ether. The product was isolated by column chromatography to afford a pink solid. Yield: 13.6 g, 68 %; m.p. 132 – 134 °C; ^{1}H NMR (250 MHz, $CDCl_3$, 25 °C, TMS): $\delta = 7.35 – 7.30$ (m, 5H), 6.68 (s, 4H), 5.03 (s, 2H), 3.32 (brs, 4H), 2.50 – 2.45 (brm, 4H), 2.15 – 2.10 (brm, 4H), 2.00 (s, 12H); ^{13}C NMR (250 MHz, [D$_6$]DMSO, 25 °C): $\delta = 154.7, 141.7, 137.3, 134.9, 128.5, 127.9, 127.5, 126.1, 120.4, 66.1, 42.1, 41.2, 35.6, 18.2$; FAB MS: *m/z*: 457 $[M]^+$; elemental analysis calcd (%) for $C_{29}H_{35}N_3O_2$: C 74.12, H 7.71, N 9.18; found C 74.48, H 7.61, N 8.82.

(1-Benzyloxycarbonyl)-*N*-(9-anthranoylcarboxy)-[4,4-bis(4-amino-3,5-dimethylphenyl)]piperidine (24): Compound **24** was prepared by the standard amide coupling procedure with 9-anthracene carboxylic acid (0.50 g, 2.24 mmol) in CH_2Cl_2 (50 mL), **23** (5.20 g, 11.2 mmol) and triethylamine (1.13 g, 11.2 mmol). The reaction mixture was washed with 1M HCl to remove excess **23**, which was recovered. Purification by column chromatography gave a pale yellow solid. Yield: 0.85 g, 60 %; m.p. 150 – 152 °C; ^{1}H NMR (250 MHz, $CDCl_3$, 25 °C, TMS): $\delta = 8.48$ (s, 1H), 8.30 (d, ^3J(H,H) = 8 Hz, 1H), 8.02 (d, ^3J(H,H) = 7 Hz, 1H), 7.50 (m, 4H), 7.30 (m, 5H), 7.01 (s, 2H), 6.84 (s, 2H), 5.07 (s, 2H), 3.60 (brs, 2H), 3.45 – 3.30 (brm, 4H), 2.46 (s, 6H), 2.30 – 2.10 (brm, 4H), 2.16 (s, 6H); ^{13}C NMR (250 MHz, [D$_6$]DMSO, 25 °C): $\delta = 167.8, 155.4, 147.0, 140.7, 136.9, 134.9, 134.7, 131.9, 131.4, 128.6, 128.4, 128.3, 127.9, 127.7, 127.1, 127.0, 126.8, 125.5, 125.1, 121.8, 66.9, 43.5, 41.1, 36.0, 20.0, 18.1$; FAB MS: *m/z*: 662 $[M+H]^+$; HRMS-FAB: *m/z*: 662.3319 (calcd for $C_{44}H_{44}N_3O_3$ 662.3382).

(1-Benzyloxycarbonyl)-*N*-(9-anthranoylcarboxy)-*N*′-(4-nitropyrrole-2-carboxy)-[4,4-bis(4-amino-3,5-dimethylphenyl)]piperidine (25): Compound **25** was prepared by the standard amide coupling procedure with 4-nitropyrrole-2-carboxylic acid (0.28 g, 1.84 mmol) in CH_2Cl_2 (40 mL), **24** (1.1 g, 1.67 mmol) and pyridine (0.15 g, 1.90 mmol). Purification by medium pressure column chromatography gave a pale yellow solid. Yield: 1.1 g, 85 %; m.p. 204 – 206 °C; ^{1}H NMR (250 MHz, [D$_6$]DMSO, 25 °C, TMS): $\delta =$ 12.85 (s, 1H), 10.15 (s, 1H), 9.63 (s, 1H), 8.71 (s, 1H), 8.21 (d, ^3J(H,H) = 8 Hz, 2H), 8.16 (d, ^3J(H,H) = 8 Hz, 2H), 7.95 (s, 1H), 7.65 – 7.55 (m, 5H), 7.35 – 7.30 (m, 5H), 7.18 (s, 2H), 7.15 (s, 2H), 5.05 (s, 2H), 3.60 – 3.40 (brm, 4H), 2.60 – 2.30 (brm, 4H), 2.43 (s, 6H), 2.14 (s, 6H); ^{13}C NMR (250 MHz, [D$_6$]DMSO, 25 °C): $\delta = 167.3, 155.0, 145.5, 145.3, 137.5, 136.8, 135.9, 135.5,$

133.7, 133.2, 131.2, 128.2, 127.9, 127.0, 126.8, 126.5, 126.1, 66.6, 43.8, 20.0, 19.1; FAB MS: *m/z*: 800 $[M+H]^+$; HRMS-FAB: *m/z*: 800.3460 (calcd for $C_{49}H_{46}N_5O_6$ 800.3448).

[1-(3,4,5-Tri-*O*-tetradecane)-benzoyl]-*N*-(9-anthranoylcarboxy)-*N'*-(4-nitropyrrole-2-carboxy)-[4,4-bis(4-amino-3,5-dimethylphenyl)]piperidine (18): Compound **18** was prepared by the standard piperidine deprotection procedure with **25** (1.4 g, 1.75 mmol) in CH_2Cl_2 (300 mL) and TMSI (0.6 mL). The solubilising group was added by using **21** (1.46 g, 1.91 mmol), EDC (0.40 g, 2.10 mmol) and HOBt (0.28 g, 2.10 mmol). Purification by column chromatography afforded a pale yellow waxy solid. Yield: 0.97 g, 40%; ^{1}H NMR (250 MHz, $CDCl_3$, 0.0095 M, 25 °C, TMS): $\delta = 10.42$ (s, 1H), 8.51 (s, 1H), 8.30 (d, ^3J(H,H) = 7 Hz, 2H), 8.04 (d, ^3J(H,H) = 7 Hz, 2H), 7.61 (s, 1H), 7.51 (m, 4H), 7.57 (s, 1H), 7.28 (s, 1H), 7.31 (s, 1H), 7.07 (s, 2H), 6.99 (s, 2H), 6.56 (s, 2H), 3.95 (m, 6H), 3.80–3.40 (br m, 4H), 2.50–2.20 (br m, 4H), 2.50 (s, 6H), 2.18 (s, 6H), 1.80–1.50, 1.50–1.0 (br m, 72H), 0.95–0.80 (m, 6H); ^{13}C NMR (250 MHz, [D$_6$]DMSO, 25 °C): $\delta = 170.5$, 168.2, 158.3, 145.4, 139.2, 137.5, 135.7, 135.3, 131.8, 131.3, 131.0, 128.7, 128.2, 127.1, 126.9, 126.6, 125.6, 125.5, 124.8, 105.3, 73.5, 69.2, 44.2, 32.9, 30.3, 29.7, 29.6, 29.4, 29.3, 26.1, 22.6, 20.0, 18.7. 14.1; FAB MS: *m/z*: 1405 $[M]^+$; HRMS-FAB: *m/z*: 1406.9712 (calcd for $C_{90}H_{128}N_5O_8$ 1406.9762).

(1-Benzyloxycarbonyl)-*N*-(4-nitropyrrole-2-carboxy)-[4,4-bis(4-amino-3,5-dimethylphenyl)]piperidine (29): Compound **29** was prepared by the standard amide coupling procedure with 4-nitropyrrole-2-carboxylic acid (0.75 g, 4.80 mmol) in CH_2Cl_2 (50 mL), **23** (10.99 g, 24.0 mmol) and pyridine (0.57 g, 7.20 mmol). The product was isolated form the excess **23** by column chromatography followed by medium pressure column chromatography to give a colourless solid. Yield: 2.15 g, 75%; m.p. 158–160 °C; ^{1}H NMR (250 MHz, [D$_6$]DMSO, 25 °C, TMS): $\delta = 12.90$ (s, 1H), 9.61 (s, 1H), 7.97 (s, 1H), 7.65 (s, 1H), 7.36 (m, 5H), 7.04 (s, 2H), 6.80 (s, 2H), 5.07(s, 2H), 3.48 (br s, 2H), 3.36 (br m, 4H), 2.31 (br m, 4H), 2.13 (s, 6H), 2.06 (s, 6H); ^{13}C NMR (250 MHz, [D$_6$]DMSO, 25 °C): $\delta = 158.2$, 155.0, 147.1, 142.1, 137.5, 136.8, 135.5, 133.1, 132.1, 128.8, 128.2, 127.9, 127.0, 126.6, 126.3, 121.0, 66.5, 43.1, 35.6, 18.9, 18.6; FAB MS: *m/z*: 595 $[M]^+$; HRMS-FAB: *m/z*: 595.2835 (calcd for $C_{34}H_{37}N_5O_5$ 595.2794).

(1-Benzyloxycarbonyl)-*N*-acetyl-*N'*-(4-nitropyrrole-2-carboxy)-[4,4-bis(4-amino-3,5-dimethylphenyl)]piperidine (30): Compound **29** (0.84 g, 1.41 mmol), glacial acetic acid (0.42 g, 7.0 mmol) and EDC (1.35 g, 7.0 mmol) were dissolved in CH_2Cl_2 (50 mL) and stirred for 16 h. The reaction mixture was washed with 1 M HCl to remove most of any excess **29**, and the solvent removed under reduced pressure. The product was isolated by column chromatography to give a colourless solid. Yield: 0.68g, 76%; m.p. 185–188 °C; ^{1}H NMR (250 MHz, [D$_6$]DMSO, 25 °C, TMS): $\delta = 12.92$ (br s, 1H), 9.61 (s, 1H), 9.12 (s, 1H), 7.98 (s, 1H), 7.64 (s, 1H), 7.35 (m, 5H), 7.12 (s, 2H), 7.05 (s, 2H), 5.07 (s, 2H), 3.50–3.35 (m, 4H), 2.40–2.30 (m, 4H), 2.15 (s, 6H), 2.10 (s, 6H), 2.02 (s, 3H); ^{13}C NMR (250 MHz, [D$_6$]DMSO, 25 °C): $\delta = 167.7$, 127.7, 124.5, 144.9, 144.3, 137.0, 136.3, 135.4, 134.9, 133.2, 132.0, 127.7, 126.5, 126.0, 125.7, 125.6, 66.0, 22.5, 18.5, 18.4; FAB MS: *m/z*: 638 $[M+H]^+$; HRMS-FAB: *m/z*: 638.3002 (calcd for $C_{36}H_{40}N_5O_6$ 638.2978).

[1-(3,4,5-Tri-*O*-tetradecane)benzoyl]-*N*-acetyl-*N'*-(4-nitropyrrole-2-carboxy)-[4,4-bis(4-amino-3,5-dimethylphenyl)]piperidine (26): Compound **26** was prepared by the standard piperidine deprotection procedure with **30** (0.38 g, 0.59 mmol) in CH_2Cl_2 (70 mL) and TMSI (0.15 mL). The solubilising group was added by using **21** (0.67 g, 0.89 mmol), EDC (0.22 g, 1.18 mmol) and HOBt (0.16 g, 1.20 mmol). Purification by column chromatography afforded a pale yellow waxy solid. Yield: 0.74 g, 60%; ^{1}H NMR (250 MHz, $CDCl_3$, 0.0036 M, 25 °C, TMS): $\delta = 10.53$ (br s), 10.34 (br s, 1H), 7.70 (s, 1H), 7.32 (s, 1H), 7.30 (s, 1H), 6.98 (s, 2H), 6.93 (s, 2H), 6.65 (s, 1H), 6.53 (s, 2H), 3.95–3.90 (m, 6H), 3.90–3.60 (br m, 4H), 2.19, 2.18, 2.20 (s, 15H), 2.30–2.20 (br m, 4H), 1.90–1.70, 1.50–1.35, 1.35–1.20 (br m, 72H), 0.90–0.80 (m, 6H); ^{13}C NMR (250 MHz, $CDCl_3$, 25 °C): $\delta = 170.4$, 168.9, 158.3, 139.2, 137.5, 135.7, 135.6, 132.0, 130.8, 130.6, 126.6, 126.5, 125.6, 105.3, 73.5, 69.2, 44.1, 31.9, 30.2, 29.7, 29.7, 29.6, 29.4, 29.3, 26.0, 23.1, 22.6, 18.8, 14.1; FAB MS: *m/z*: 1244 $[M+H]^+$; elemental analysis calcd (%) for $C_{77}H_{121}N_5O_8$: C 74.29, H 9.79, N 5.25; found C 74.11, H 10.12, N 5.25.

***N,N'*-Bis-methyl isophthaldiamide (27)**: Methylamine (10.8 mL, 2 M solution in tetrahydrofuran, 22 mmol) was added dropwise to isophthaloyl dichloride (2.0 g, 9.85 mmol) in CH_2Cl_2 (100 mL), and the reaction was stirred for 10–15 minutes. After this time, a colourless precipitate began to form. The reaction mixture was reduced in volume on a rotary evaporator, and the resultant colourless precipitate was filtered and washed repeatedly with CH_2Cl_2 and petroleum ether to afford a colourless solid. Yield: 1.7 g, 90%; m.p. 169–171 °C; ^{1}H NMR (250 MHz, [D$_6$]DMSO, 25 °C, TMS): $\delta =$ 8.90 (s, 2H), 8.55 (s, 1H), 8.14 (d, ^3J(H,H) = 8 Hz, 2H), 8.09 (s, 4H), 7.65 (t, ^3J(H,H) = 8 Hz, 1H), 2.90 (s, 6H); ^{13}C NMR (250 MHz, [D$_6$]DMSO, 25 °C): $\delta = 166.2$. 134.5. 129.6. 128.4. 126.1. 26.3. 24.1; FAB MS: *m/z*: 192 $[M]^+$.

***N*-(4-Nitropyrrole-2-carboxy)-{1,1-bis[(4-amino-3,5-dimethyl)phenyl]cyclohexane} (31)**: Compound **31** was prepared by using the standard amide coupling procedure with 4-nitro-pyrrole-2-carboxylic acid (1.0 g, 6.41 mmol) in CH_2Cl_2 (40 mL), bisaniline **16** (6.19 g, 19.2 mmol) and pyridine (0.55 g, 7.05 mmol). Purification by column chromatography afforded a yellow solid. Yield: 0.65g, 22%; m.p. 188–190 °C; ^{1}H NMR (250 MHz, [D$_6$]DMSO, 25 °C, TMS): $\delta = 12.89$ (s, 1H), 9.58 (s, 1H), 7.96 (s, 1H), 7.63 (s, 1H), 7.00 (s, 2H), 6.76 (s, 2H), 4.33 (br s, 2H), 2.30–2.00 (m, 4H), 2.11 (s, 6H), 2.04 (s, 6H), 1.6–1.4 (br m, 6H); ^{13}C NMR (250 MHz, [D$_6$]DMSO, 25 °C): $\delta = 158.7$, 149.5, 140.1, 137.5, 134.8, 129.4, 127.1, 127.0, 125.6, 121.6, 105.1, 44.9, 37.1, 26.4, 22.9, 18.8, 18.0; FAB MS: *m/z*: 460 $[M]^+$; elemental analysis calcd (%) for $C_{27}H_{32}N_4O_3 \cdot 0.25\,H_2O$: C 69.73, H 7.04, N 11.72; found C 69.95, H 7.10, N 12.05.

***N*-(4-Nitropyrrole-2-carboxy)-*N'*-acetyl-{1,1-bis[(4-amino-3,5-dimethyl)-phenyl]cyclohexane} (31)**: Compound **32** (1.0 g, 2.17 mmol) and glacial acetic acid (0.13 g, 2.20 mmol) were suspended in CH_2Cl_2 (40 mL). EDC (0.54 g, 2.82 mmol) was added, and the reaction mixture was stirred for 12 h. It was then washed with 1 M HCl and water, and the solvent was removed under reduced pressure. The product was isolated by column chromatography to give a colourless solid. Yield: 0.64 g, 59%; m.p. >250 °C; ^{1}H NMR (250 MHz, [D$_6$]DMSO, 25 °C, TMS): $\delta = 12.90$ (br s, 1H), 9.54 (s, 1H), 9.04 (s, 1H), 7.92 (s, 1H), 7.58 (s, 1H), 7.05 (s, 2H), 6.98 (s, 2H), 2.30–2.00 (m, 4H), 2.20 (m, 4H), 2.11 (s, 6H), 2.07 (s, 6H), 1.99 (s, 3H), 1.6–1.4 (br m, 6H); ^{13}C NMR (250 MHz, [D$_6$]DMSO, 25 °C): $\delta =$ 167.2, 147.2, 146.5, 136.8, 135.5, 135.0, 133.2, 126.6, 126.3, 45.1, 36.5, 23.0, 19.0; FAB MS: *m/z*: 503 $[M+H]^+$; elemental analysis calcd (%) for $C_{29}H_{34}N_4O_4 \cdot H_2O$: C 66.90, H 6.97, N 10.76; found C 66.89, H 6.82, N 10.65.

(1-Benzyloxycarbonyl)-*N*-(4-nitropyrrole-2-carboxy)-*N'*-pentafluorobenzoyl-[4,4-bis(4-amino-3,5-dimethylphenyl)]piperidine (34): The monosubstituted bisaniline was synthesised by the standard amide coupling procedure by reaction of pentafluorobenzoyl chloride (3.28 g, 14.2 mmol), **23** (13.8 g, 43.7 mmol) and triethylamine (2.16 g, 21.4 mmol), but was not isolated as it contained a lot of the diaddition product and was difficult to separate at this stage. Therefore the mixture was treated with 4-nitropyrrole-2-carbonyl chloride **15** (0.53 g, 3.40 mmol) and pyridine (0.40 g, 5.1 mmol) by using the standard procedure and the products separated after this step. The product was isolated by medium-pressure column chromatography to give a colourless solid. Yield: 6.73 g, 60%; m.p. 187–189 °C; ^{1}H NMR (250 MHz, [D$_6$]DMSO, 25 °C, TMS): $\delta = 12.92$ (s, 1H), 10.28 (s, 1H), 9.62 (s, 1H), 7.98 (s, 1H), 7.64 (s, 1H), 7.35 (m, 5H), 7.16 (s, 2H), 7.15 (s, 2H), 5.08 (s, 2H), 3.45 (br m, 4H), 2.40 (br m, 4H), 2.21 (s, 6H), 2.16 (s, 6H); ^{13}C NMR (250 MHz, [D$_6$]DMSO, 25 °C): $\delta = 145.2$, 137.4, 136.8, 135.9, 135.2, 132.5, 131.8, 128.8, 128.2, 127.9, 126.9, 126.7, 66.5, 43.9, 18.9, 18.7; ^{19}F NMR ($CDCl_3$) $\delta = -141$, -151, -160; FAB MS: *m/z*: 790 $[M+H]^+$; HRMS-FAB: *m/z*: 790.2708 (calcd for $C_{41}H_{37}F_5N_5O_6$ 790.2664).

1-(3,4,5-Tri-*O*-tetradecane)benzoyl)-*N*-(4-nitropyrrole-2-carboxy)-*N'*-pentafluorobenzoyl-[4,4-bis(4-amino-3,5-dimethylphenyl)]piperidine (33): Compound **33** was prepared by the standard piperidine deprotection procedure with **34** (0.99 g, 1.25 mmol) in CH_2Cl_2 (150 mL) and TMSI (0.5 mL). The solubilising group was added by using **21** (1.14 g, 1.50 mmol), EDC (0.28 g, 1.50 mmol) and HOBt (0.20 g, 1.50 mmol). Purification by column chromatography gave a colourless waxy solid. Yield: 0.95 g, 70%; ^{1}H NMR (250 MHz, $CDCl_3$, 0.0014 M, 25 °C, TMS): $\delta = 9.98$ (br s, 1H), 9.83 (s), 7.45 (s, 1H), 7.18 (s, 1H), 7.09 (s, 1H), 7.00 (s, 2H), 6.99 (s, 2H), 6.54 (s, 2H), 5.33 (s), 3.95–3,90 (m, 6H), 3.80–3.40 (br m, 4H), 2.50–2.30 (br m), 2.28 (s, 6H), 2.22 (s, 6H), 1.85–1.60, 1.60–1.10 (m, 72H), 0.95–0.85 (m, 9H); ^{13}C NMR (250 MHz, [D$_6$]DMSO, 25 °C): $\delta = 170.4$, 158.1, 155.9, 153.2, 146.5, 145.8, 139.3, 137.8, 135.7, 130.6, 126.9, 126.7, 125.5, 105.4, 73.5, 69.2, 44.3, 31.9. 30.3, 29.7, 29.6, 29.4, 29.3, 26.1, 22.6, 18.8, 14.0; ^{19}F NMR ($CDCl_3$) $\delta = -142$, -150, -163; FAB MS: *m/z*: 1395 $[M]^+$; HRMS-FAB: *m/z*: 1396.8863 (calcd for $C_{82}H_{119}F_5N_5O_8$ 1396.8978); elemental analysis calcd (%) for $C_{82}H_{118}F_5N_5O_8$: C 70.50, H 8.51, N 5.01; found C 70.27, H 8.61, N 4.95.

0947-6539/01/0722-4876 $ 17.50+.50/0 *Chem. Eur. J.* **2001**, *7*, No. 22

Crystal structure data: Crystallographic data (excluding structure factors) for the structures reported in this paper have been deposited with the Cambridge Crystallographic Data Centre as supplementary publication nos. CCDC-162594 to 162598. Copies of this data can be obtained free of charge on application to CCDC, 12 Union Road, Cambridge CB2 1EZ, UK (fax: (+44) 1223-336033; e-mail: deposit@ccdc.cam.ac.uk).

Compound 8: $C_{27}H_{25}NO$; $M = 379.48$. Crystallises from petroleum ether/CH_2Cl_2 as pale yellow blocks. Crystal dimensions $0.40 \times 0.18 \times 0.10$ mm; monoclinic, $a = 20.611(2)$, $b = 13.4661(14)$, $c = 26.000(3)$ Å, $\beta = 111.789(3)^\circ$ $U = 6700.8(12)$ Å^3, $Z = 12$, $D_c = 1.128$ Mg m^{-3}, space group $P2_1/n$ (a non standard setting of $P2_1/c$ C_{2h}^5 No. 14), Mo-K_α radiation ($\lambda = 0.71073$ Å), μ(Mo-K_α) = 0.068 mm^{-1}, $F(000) = 2424$.

Compound 9: $C_{23}H_{19}NO$; $M = 325.39$. Crystallises from CH_2Cl_2 as colourless blocks. Crystal dimensions $0.68 \times 0.42 \times 0.32$ mm; monoclinic, $a = 16.604(3)$, $b = 4.6310(9)$, $c = 23.722(5)$ Å, $\beta = 108.08(3)^\circ$, $U = 1734.0(6)$ Å^3, $Z = 4$, $D_c = 1.246$ Mg m^{-3}, space group $P2_1/c$ (C_{2h}^5 No. 14), Mo-K_α radiation ($\lambda = 0.71073$ Å), μ(Mo-K_α) = 0.076 mm^{-1}, $F(000) = 688$.

Compound 10: $C_{21}H_{10}F_5NO$; $M = 387.30$. Crystallises from petroleum ether/CH_2Cl_2 as colourless blocks. Crystal dimensions $0.4 \times 0.1 \times 0.1$ mm; monoclinic, $a = 14.100(3)$, $b = 13.585(3)$, $c = 18.372(4)$ Å, $\beta = 108.308(4)^\circ$, $U = 3341.0(12)$ Å^3, $Z = 8$, $D_c = 1.540$ Mg m^{-3}, space group $P2_1/n$ (a non standard setting of $P2_1/c$ C_{2h}^5 No. 14), Mo-K_α radiation ($\lambda = 0.71073$ Å), μ(Mo-K$_\alpha$) = 0.133 mm^{-1}, $F(000) = 1568$.

Compound 25: $C_{53.5}H_{45}Cl_9N_5O_{7.5}$; $M = 1196.99$. Crystallises from petroleum ether/CH_2Cl_2 as colourless blocks. Crystal dimensions $0.39 \times 0.38 \times 0.36$ mm; monoclinic, $a = 22.82(2)$, $b = 21.214(18)$, $c = 25.75(2)$ Å, $\beta = 106.49(13)^\circ$, $U = 11949(19)$ Å^3, $Z = 8$, $D_c = 1.331$ Mg m^{-3}, space group $C2/c$, Mo-K_α radiation ($\lambda = 0.71073$ Å), μ(Mo-K_α) = 0.474 mm^{-1}, $F(000) = 4912$.

Compound 31: $C_{30}H_{36}Cl_2N_4O_4$; $M = 587.53$. Crystallises from petroleum ether/CH_2Cl_2 as colourless blocks. Crystal dimensions $0.45 \times 0.20 \times 0.20$ mm; triclinic, $a = 9.368(2)$, $b = 11.533(3)$, $c = 27.828(7)$ Å, $\alpha = 97.545(5)^\circ$ $\beta = 92.026(5)^\circ$, $\gamma = 92.943(5)^\circ$, $U = 2974.0(12)$ Å^3, $Z = 4$, $D_c = 1.312$ Mg m^{-3}, space group $P\bar{1}$ (C_i^1 No. 2), Mo-K_α radiation ($\lambda = 0.71073$ Å), μ(Mo-K_α) = 0.260 mm^{-1}, $F(000) = 1240$.

Acknowledgement

We thank the Lister Institute (C.A.H.), EPSRC (J.P.), BBSRC (J.M.S.) and Zeneca Agrochemicals (J.P.) for financial support.

[1] C. A. Hunter, J. K. M. Sanders, *J. Am. Chem. Soc.* **1990**, *112*, 5525–5534.
[2] J. D. Watson, F. H. Crick, *Nature* **1953**, *171*, 737–738.
[3] W. Saenger, *Principles of Nucleic Acid Structure* Springer, New York, **1988**.
[4] C. A. Hunter, *J. Mol. Biol.* **1993**, *230*, 1025–1054.
[5] S. K. Burley, G. A. Petsko, *Science* **1985**, 23–28.
[6] C. A. Hunter, *Chem. Soc. Rev.* **1994**, *23*, 101–109.
[7] L. S. Lerman, *J. Mol. Biol.* **1961**, *3*, 18–30.
[8] P. L. Anelli, N. Spencer, J. F. Stoddart, *J. Am. Chem. Soc.* **1991**, *113*, 5131–5133.
[9] A. D. Hamilton, D. Van Engen, *J. Am. Chem. Soc.* **1987**, *109*, 5035–5036.
[10] S. B. Ferguson, F. Diederich, *Angew. Chem.* **1986**, *98*, 1127–1129; *Angew. Chem. Int. Ed. Engl.* **1986**, *25*, 1127–1129.
[11] B. J. Whitlock, H. W. Whitlock, *J. Am. Chem. Soc.* **1990**, *112*, 3910–3915.
[12] J. Rebek, D. Nemeth, *J. Am. Chem. Soc.* **1986**, *108*, 5637–5638.
[13] H. J. Schneider, T. Blatter, S. Simova, I. Theis, *Chem. Commun.* **1989**, 580–581.
[14] A. W. Schwabacher, S. Zhang, W. Davy, *J. Am. Chem. Soc.* **1993**, *115*, 6995–6996.
[15] J. S. Zhang, J. S. Moore, *J. Am. Chem. Soc.* **1992**, *114*, 9701–9702.
[16] S. C. Zimmerman, C. M. Vanzyl, *J. Am. Chem. Soc.* **1987**, *109*, 7894–7896.
[17] S. C. Zimmerman, C. M. Vanzyl, G. S. Hamilton, *J. Am. Chem. Soc.* **1989**, *111*, 1373–1381.
[18] S. C. Zimmerman, W. S. Kwan, *Angew. Chem.* **1995**, *107*, 2404–2406; *Angew. Chem. Int. Ed. Engl.* **1995**, *34*, 2404–2406.
[19] J. N. H. Reek, A. Kros, R. J. M. Nolte, *Chem. Commun.* **1996**, 245–247.
[20] J. C. Ma, D. A. Dougherty, *Chem. Rev.* **1997**, *97*, 1303–1324.
[21] G. R. Desiraju, A. Gavezzotti, *Acta. Cryst. B* **1989**, *45*, 473–482.
[22] G. R. Desiraju, A. Gavezzotti, *Chem. Commun.* **1989**, 621–623.
[23] G. W. Coates, A. R. Dunn, L. M. Henling, D. A. Dougherty, R. H. Grubbs, *Angew. Chem.* **1997**, *109*, 290–293; *Angew. Chem. Int. Ed. Engl.* **1997**, *36*, 248–251.
[24] G. W. Coates, A. R. Dunn, L. M. Henling, J. W. Ziller, E. B. Lobkovsky, R. H. Grubbs, *J. Am. Chem. Soc.* **1998**, *120*, 3642–3649.
[25] P. Linse, *J. Am. Chem. Soc.* **1992**, *114*, 4366–4373.
[26] W. L. Jorgensen, D. L. Severance, *J. Am. Chem. Soc.* **1990**, *112*, 4768–4774.
[27] R. L. Jaffe, G. D. Smith, *J. Chem. Phys.* **1996**, *105*, 2780–2788.
[28] R. L. Jaffe, G. D. Smith, *J. Phys. Chem.* **1996**, *100*, 9624–9630.
[29] C. Chipot, R. Jaffe, B. Maigret, D. A. Pearlman, P. A. Kollman, *J. Am. Chem. Soc.* **1996**, *118*, 11217–11224.
[30] P. Hobza, H. L. Selzle, E. W. Schlag, *J. Phys. Chem.* **1993**, *97*, 3937–3938.
[31] P. Hobza, H. L. Selzle, E. W. Schlag, *J. Am. Chem. Soc.* **1994**, *116*, 3500–3506.
[32] S. L. Price, A. J. Stone, *J. Chem. Phys.* **1987**, *86*, 2859–2868.
[33] F. Cozzi, F. Ponzini, R. Annunziata, M. Cinquini, J. S. Siegel, *Angew. Chem.* **1995**, *107*, 1092–1093; *Angew. Chem. Int. Ed. Engl.* **1995**, *34*, 1019–1020.
[34] F. Cozzi, M. Cinquini, R. Annunziata, J. S. Siegel, *J. Am. Chem. Soc.* **1993**, *115*, 5330–5331.
[35] S. Paliwal, S. Geib, C. S. Wilcox, *J. Am. Chem. Soc.* **1994**, *116*, 4497–4498.
[36] E. Kim, S. Paliwal, C. S. Wilcox, *J. Am. Chem. Soc.* **1998**, *120*, 11192–11193.
[37] L. F. Newcomb, S. H. Gellman, *J. Am. Chem. Soc.* **1994**, *116*, 4993–4994.
[38] N. J. Heaton, P. Bello, B. Herrandon, A. del Campo, J. Jiminez-Barbero, *J. Am. Chem. Soc.* **1998**, *120*, 12371–12384.
[39] M. J. Packer, C. A. Hunter, *J. Mol. Biol.* **1998**, *280*, 407–420.
[40] M. J. Packer, M. P. Dauncey, C. A. Hunter, *J. Mol. Biol.* **2000**, *295*, 71–83.
[41] M. J. Packer, M. P. Dauncey, C. A. Hunter, *J. Mol. Biol.* **2000**, *295*, 85–103.
[42] L. Serrano, M. Bycroft, A. R. Fersht, *J. Mol. Biol.* **1991**, *218*, 465–475.
[43] H. Adams, F. J. Carver, C. A. Hunter, J. C. Morales, E. M. Seward, *Angew. Chem.* **1996**, *108*, 1628–1631; *Angew. Chem. Int. Ed. Engl.* **1996**, *35*, 1542–1544.
[44] A. P. Bisson, F. J. Carver, C. A. Hunter, J. P. Waltho, *J. Am. Chem. Soc.* **1994**, *116*, 10292–10293.
[45] A. P. Bisson, C. A. Hunter, *Chem. Commun.* **1996**, 1723–1724.
[46] F. J. Carver, C. A. Hunter, P. S. Jones, D. J. Livingstone, J. F. McCabe, E. M. Seward, P. Tiger, *Chem. Eur. J.* **2001**, *7*, 4854–4862.
[47] C. R. Patrick, G. S. Prosser, *Nature* **1960**, 1021.
[48] T. Dahl, *Acta. Chem. Scan. A* **1975**, *29*, 170–174.
[49] H. Adams, K. D. M. Harris, G. A. Hembury, C. A. Hunter, D. Livingstone, J. F. McCabe, *Chem. Commun.* **1996**, 2531–2532.
[50] K. J. Morgan, D. P. Morrey, *Tetrahedron* **1966**, *22*, 57–62.
[51] P. E. Fanta, *Org. Synth.* **1952**, *32*, 95–96.
[52] C. A. Hunter, *J. Am. Chem. Soc.* **1992**, *114*, 5303–5311.
[53] R. S. Lott, V. S. Chauhan, C. H. Stammer, *Chem. Commun.* **1979**, 495–496.
[54] C. A. Hunter, M. J. Packer, *Chem. Eur. J.* **1999**, *5*, 1891–1897.
[55] J. Vrbancich, G. L. D. Ritchie, *J. Chem. Soc. Faraday Trans. II* **1980**, *76*, 648–659.
[56] M. Gardner, A. J. Guerin, C. A. Hunter, U. Michelsen, C. Rotger, *New J. Chem.* **1999**, 309–316. Note in Equation (6) of this paper, the factor of 2 should be absent.
[57] A. P. Bisson, C. A. Hunter, J. C. Morales, K. Young, *Chem. Eur. J.* **1998**, *4*, 845–851.

Received: May 7, 2001 [F3238]

0947-6539/01/0722-4878 $ 17.50+.50/0